JAERI-M
9466

STABILITY ANALYSIS OF INTOR

(IAEA INTOR WORKSHOP REPORT PHASE I, PHYSICS (1))

April 1981

Tatsuoki TAKEDA, Kimitaka ITOH, Masafumi AZUMI
Gen-ichi KURITA, Tomonori TAKIZUKA, Shinji TOKUDA
Toshihide TSUNEMATSU, Takashi TUDA, Sanae-Inoue
ITOH* Toshihiko MATSUURA**and Yukio TANAKA**

日本原子力研究所
Japan Atomic Energy Research Institute

この報告書は，日本原子力研究所が JAERI-M レポートとして，不定期に刊行している研究報告書です．入手，複製などのお問合わせは，日本原子力研究所技術情報部（茨城県那珂郡東海村）あて，お申しこしください．

JAERI-M reports, issued irregularly, describe the results of research works carried out in JAERI. Inquiries about the availability of reports and their reproduction should be addressed to Division of Technical Information, Japan Atomic Energy Research Institute, Tokai-mura, Naka-gun, Ibaraki-ken, Japan.

JAERI-M 9466

Stability Analysis of INTOR

[IAEA INTOR Workshop Report
Phase I, Physics [1]]

Tatsuoki TAKEDA, Kimitaka ITOH, Masafumi AZUMI
Gen-ichi KURITA, Tomonori TAKIZUKA, Shinji TOKUDA,
Toshihide TSUNEMATSU, Takashi TUDA, Sanae-Inoue ITOH*
Toshihiko MATSUURA** and Yukio TANAKA**

Division of Thermonuclear Fusion Research,
Tokai Research Establishment, JAERI

(Received April 6, 1981)

Stability of the INTOR plasma is investigated from various viewpoints. Instabilities considered in this article are positional instability, low-n kink and internal mode instabilities, high-n ballooning mode instability and resistive instability. Considering that the high-n ballooning mode instability is very important from the viewpoint of the beta optimization it is investigated minutely. Possibility of attaining a very high beta equilibrium in the second stable region of the ballooning instability is presented.

Both the MHD and kinetic approaches are adopted to understand the behavior of the INTOR plasma comprehensively.

Keywords: Stability Analysis, Tokamak, INTOR, Beta Limit, Positional Instability, Kink Mode Instability, Ballooning Mode Instability, Resistive Instability

---

* Institute for Fusion Theory, Hiroshima University, Hiroshima

** Fujitsu Ltd., Shinkamata, Ohta, Tokyo

JJAERI-M 9466

INTORの安定性解析

(IAEA INTORワークショップ報告書 フェイズI, 物理〔1〕)

日本原子力研究所東海研究所核融合研究部
竹田 辰興・伊藤 公孝・安積 正史・栗田 源一
滝塚 知典・徳田 伸二・常松 俊秀・津田 孝
伊藤 早苗*・松浦 俊彦**・田中 幸夫**

(1981年4月6日受理)

種々の観点からINTORプラズマの安定性を調べた。本報告書で考えられている不安定性は，位置不安定性，低nキンク・モード，低n内部不安定性，高nバルーニング・モード不安定性および抵抗性不安定性である。ベータ値最適化の点からバルーニング・モード不安定性が重要であることを考えて，これについては詳しく調べた。バルーニング不安定性の第2安定領域に存在する非常にベータ値の高い平衡の実現可能性も示した。

INTORプラズマの挙動を包括的に理解するためにMHD的および粒子運動論的手法の両方を用いて解析が行われた。

* 広島大学 核融合理論研究センター

** 富士通(株)

Contents

目　　次

1. Introduction

In designing a new tokamak device it is needless to say that macroscopic behavior of a plasma should be first investigated. This kind of investigations include linearized or nonlinear, and ideal or dissipative MHD analyses which are, sometimes, approached directly from the kinetic theory. From the viewpoint of performance of the device the maximum attainable beta value is the most important parameter to be considered in designing the device and, presently, the detailed analysis of MHD instabilities is almost the only method to estimate the beta value. In this connection the above analysis is indispensable to determine the configurational or physical parameters of the device which realize the optimized performance. Nonlinear analyses of the plasma give us important informations on disruptive instabilities or other deteriorative plasma behavior.

In our program of analyses of the INTOR plasma[1] we investigate the above phenomena as comprehensively as possible. The phenomena we investigate are positional instability, low-n kink mode instability, low-n internal mode instability, high-n ballooning mode instability, and resistive instability. As the high-n ballooning mode instability is very important to asses the maximum attainable beta value, we investigate it very minutely. In this analysis the finite-n correction and kinetic effect are taken into account. We present a result of analysis on a tearing mode instability by the kinetic theory and a result of numerical analysis on formation of large-scale magnetic island due to a resistive internal mode. No conclusions on analyses of the major disruptions are presented in this article.

2. Equilibrium

By solving the Grad-Shafranov equation two types of equilibria are prepared for the further stability calculations. One is the equilibrium derived as a solution of a nonlinear eigenvalue (pressure gradient) problem and the other is the flux conserving tokamak (FCT) equilibrium.

In the former calculation the functional forms of the pressure $P(\psi)$ and toroidal field function $T(\psi)$ are specified beforehand as

$$P(\psi) = \beta_J P_o' \{\psi - \frac{\alpha}{2}[(\psi-\psi_o)^2-\psi_o^2] + \frac{\gamma}{L+1}[(\psi-\psi_o)^{L+1}-(-\psi_o)^{L+1}]\},$$

1. Introduction

In designing a new tokamak device it is needless to say that macroscopic behavior of a plasma should be first investigated. This kind of investigations include linearized or nonlinear, and ideal or dissipative MHD analyses which are, sometimes, approached directly from the kinetic theory. From the viewpoint of performance of the device the maximum attainable beta value is the most important parameter to be considered in designing the device and, presently, the detailed analysis of MHD instabilities is almost the only method to estimate the beta value. In this connection the above analysis is indispensable to determine the configurational or physical parameters of the device which realize the optimized performance. Nonlinear analyses of the plasma give us important informations on disruptive instabilities or other deteriorative plasma behavior.

In our program of analyses of the INTOR plasma[1] we investigate the above phenomena as comprehensively as possible. The phenomena we investigate are positional instability, low-n kink mode instability, low-n internal mode instability, high-n ballooning mode instability, and resistive instability. As the high-n ballooning mode instability is very important to asses the maximum attainable beta value, we investigate it very minutely. In this analysis the finite-n correction and kinetic effect are taken into account. We present a result of analysis on a tearing mode instability by the kinetic theory and a result of numerical analysis on formation of large-scale magnetic island due to a resistive internal mode. No conclusions on analyses of the major disruptions are presented in this article.

2. Equilibrium

By solving the Grad-Shafranov equation two types of equilibria are prepared for the further stability calculations. One is the equilibrium derived as a solution of a nonlinear eigenvalue (pressure gradient) problem and the other is the flux conserving tokamak (FCT) equilibrium.

In the former calculation the functional forms of the pressure $P(\psi)$ and toroidal field function $T(\psi)$ are specified beforehand as

$$P(\psi) = \beta_J P_o' \{\psi - \frac{\alpha}{2}[(\psi-\psi_o)^2-\psi_o^2] + \frac{\gamma}{L+1}[(\psi-\psi_o)^{L+1}-(-\psi_o)^{L+1}]\},$$

$$\gamma = - \frac{1-\alpha\psi_o}{(-\psi_o)^L} \quad ,$$

$$TT' = \left(\frac{1}{\beta_J} - 1 \right) P' \frac{1}{\left\langle \frac{1}{r^2} \right\rangle} \sim \left(\frac{1}{\beta_J} - 1 \right) R_o^2 P' \quad ,$$

where ψ_0 is the flux function (ψ) at the magnetic axis, r is the major radius ($r=R_0$: position of the magnetic axis), and β_J is the approximate value of the poloidal beta. The plasma shape is specified and the calculations are carried out as a fixed boundary problem. Hereafter, we call this type "the model equilibrium #1". There are infinite possibilities to choose the functional forms of $P(\psi)$ and $T(\psi)$, and we also try to use different choice for the caluclation of high-n ballooning instabilities as

$$P(\psi) = \left(\frac{\psi-\psi_b}{\psi_o-\psi_b} \right) \quad ,$$

$$TT'(\psi) = \left(\frac{1}{\beta_J} - 1 \right) R_o^2 \, P' \quad .$$

We call it "the model equilibrium #1'".

In the case of FCT equilibrium we start from the former type of equilibria and specify the safety factor profile $q(\psi)$ according to the initial equilibria. Then we increase the plasma pressure so that

$$\frac{d}{dt} P(\psi) \left(\frac{dV}{d\psi}\right)^\gamma = S(\psi) \left(\frac{dV}{d\psi}\right)^\gamma$$

where $S(\psi)$ is the heat source profile and $\gamma = 5/3$. We solve the Grad-Shafranov equation keeping $q(\psi)$ and $P(\psi)\left(\frac{dV}{d\psi}\right)^\gamma$ constant using iterative procedure based on the combination of PDE(partial differential equation) and ODE (ordinary differential equation). As for the shape of the plasma surface several points belonging to the assumed plasma surface are specified beforehand and the corresponding number of multipole components of the vacuum magnetic field are adjusted so that the specified points are always on the plasma surface throughout the iteration process. This procedure, however, gives rise to a skin current at the plasma surface due to the difference of toroidal component of magnetic fields inside and outside the plasma. To avoid it the primary current flux is controlled and the plasma cross-section is enlarged by conserving the shape of the cross-section. We call this type "the model equilibrium #2".

The model equilibrium #1 is appropriate to study phenomena which are strongly dependent on the poloidal beta value because the approximate poloidal beta value is specified before the equilibrium calculation. By this formulation, however, we cannot get a very high beta equilibrium without a negative toroidal current. On the other hand by the FCT calculation a very high beta equilibrium is easily obtained but the poloidal beta value is not known before calculation.

3. Positional instability

Analysis of a positional instability is very important for an elongated tokamak plasma as INTOR. And stabilization of the instability should be first considered when designing a device. If one can locate a perfectly conducting wall close enough to the plasma surface the instability can be stabilized. From technological requirements, however, the distance between the plasma surface and conducting wall is restricted above a certain value and, moreover, the wall is not perfectly conducting.

For designing of INTOR the following should be studied; (i) within the framework of the linear theory if plasma equilibria with given plasma parameters are stable against the positional instability under the given external conditions such as the given wall position, and (ii) within the framework of the nonlinear theory if the above instability can be stabilized with or without a technologically realizable feedback stabilization system. In the present work, however, we only analyze the dependence of the positional instability on the wall position and elongation.[2)]

First, we study the effect of the conducting wall on the positional instability for several different shapes of a plasma cross-section by using the code ERATO[3)]. The plasma parameters are: $q_a = 2.5$, $\beta_p = 1.3$, and other parameters are standard values of the INTOR device. The growth rate of the instability is computed by varying the plasma-wall distance ($\Lambda = b/a$; b and a are the short radii of the wall and plasma, respectively) and the critical value of Λ is determined by extrapolation according to the $1 - \Lambda^{-3}$ scaling law[4)] (Fig. 3.1). The figure shows that the critical wall position Λ_c for an elliptical plasma is about 2.0, which agrees well with the result of Laval et al.[5)], $(E-1)/(E+1) = \Lambda^{-2}$. It is concluded that the plasma of INTOR can be made stable against the positional instability by locating a perfectly conducting wall at $\Lambda < 1.5$, irrespective of small triangularity or rectangularity.

The model equilibrium #1 is appropriate to study phenomena which are strongly dependent on the poloidal beta value because the approximate poloidal beta value is specified before the equilibrium calculation. By this formulation, however, we cannot get a very high beta equilibrium without a negative toroidal current. On the other hand by the FCT calculation a very high beta equilibrium is easily obtained but the poloidal beta value is not known before calculation.

3. Positional instability

Analysis of a positional instability is very important for an elongated tokamak plasma as INTOR. And stabilization of the instability should be first considered when designing a device. If one can locate a perfectly conducting wall close enough to the plasma surface the instability can be stabilized. From technological requirements, however, the distance between the plasma surface and conducting wall is restricted above a certain value and, moreover, the wall is not perfectly conducting.

For designing of INTOR the following should be studied; (i) within the framework of the linear theory if plasma equilibria with given plasma parameters are stable against the positional instability under the given external conditions such as the given wall position, and (ii) within the framework of the nonlinear theory if the above instability can be stabilized with or without a technologically realizable feedback stabilization system. In the present work, however, we only analyze the dependence of the positional instability on the wall position and elongation.[2)]

First, we study the effect of the conducting wall on the positional instability for several different shapes of a plasma cross-section by using the code ERATO[3)]. The plasma parameters are: $q_a = 2.5$, $\beta_p = 1.3$, and other parameters are standard values of the INTOR device. The growth rate of the instability is computed by varying the plasma-wall distance ($\Lambda = b/a$; b and a are the short radii of the wall and plasma, respectively) and the critical value of Λ is determined by extrapolation according to the $1 - \Lambda^{-3}$ scaling law[4)] (Fig. 3.1). The figure shows that the critical wall position Λ_c for an elliptical plasma is about 2.0, which agrees well with the result of Laval et al.[5)], $(E-1)/(E+1) = \Lambda^{-2}$. It is concluded that the plasma of INTOR can be made stable against the positional instability by locating a perfectly conducting wall at $\Lambda < 1.5$, irrespective of small triangularity or rectangularity.

Secondly, we investigate the dependence of the positional instability on the ellipticity of the plasma surface. The motivation of this study is to know whether the ellipticity of 1.5 is appropriate from the viewpoint of the positional instability. In this analysis we choose the safety factor and poloidal beta value as q_s = 4.0 and β_p=2.0. Figure 3.2 shows the growth rate of the instability vs. ellipticity for the cases with a conducting wall at Λ = 1.6 and without the conducting wall.

Conclusions from the above analyses are summarized as follows:
(1) A plasma with ellipticity less than about 1.5 is stable against the positional instability if a perfectly conducting wall is located sufficiently close to the plasma surface ($\Lambda \lesssim 1.6$).
(2) If there is no conducting wall with long skin time, a plasma with any ellipticity is unstable against the positional instability.

The above conclusions suggest that decreasing of the ellipticity of the INTOR plasma does not hlep to improve the positional stability appreciably. Remaining problems which have not been studied yet are;
(1) From our preliminary calculations it seems that triangular deformation of the plasma surface deteriorates the positional stability. This problem is related to a case with separatrices of the vacuum field, but it has not been studied yet as all the analyses of the positional instability up to now are carried out for equilibria with given shapes of a plasma surface.
(2) In our analyses it is assumed that the conducting wall completely surrounds the plasma surface, but in the actual device the conducting wall has some slits and/or holes which may deteriorate the stability. The positional stability will be worsened by taking into account this effect but it will be recovered by considering the nonlinear saturation of the mode. For the purpose of analyzing the effect we are now developing a 2-dimensional nonlinear code AEOLUS-P[6].

4. Low-n kink mode instability

A conducting wall surrounding the plasma is also effective to stabilize a low-n external kink mode instability. This was numerically confirmed by Berger et al. for the case of a tokamak with the Solov'ev equilibrium[7] and by Tsunematsu et al. for the case of a conventional circular cross-sectional tokamak with a more realistic current profile[8]. Both the calculations are carried out by using the code ERATO as in the previous section. According to the latter calculation the external n=1

Secondly, we investigate the dependence of the positional instability on the ellipticity of the plasma surface. The motivation of this study is to know whether the ellipticity of 1.5 is appropriate from the viewpoint of the positional instability. In this analysis we choose the safety factor and poloidal beta value as $q_s = 4.0$ and $\beta_p = 2.0$. Figure 3.2 shows the growth rate of the instability vs. ellipticity for the cases with a conducting wall at $\Lambda = 1.6$ and without the conducting wall.

Conclusions from the above analyses are summarized as follows:
(1) A plasma with ellipticity less than about 1.5 is stable against the positional instability if a perfectly conducting wall is located sufficiently close to the plasma surface ($\Lambda \lesssim 1.6$).
(2) If there is no conducting wall with long skin time, a plasma with any ellipticity is unstable against the positional instability.

The above conclusions suggest that decreasing of the ellipticity of the INTOR plasma does not hlep to improve the positional stability appreciably. Remaining problems which have not been studied yet are;
(1) From our preliminary calculations it seems that triangular deformation of the plasma surface deteriorates the positional stability. This problem is related to a case with separatrices of the vacuum field, but it has not been studied yet as all the analyses of the positional instability up to now are carried out for equilibria with given shapes of a plasma surface.
(2) In our analyses it is assumed that the conducting wall completely surrounds the plasma surface, but in the actual device the conducting wall has some slits and/or holes which may deteriorate the stability. The positional stability will be worsened by taking into account this effect but it will be recovered by considering the nonlinear saturation of the mode. For the purpose of analyzing the effect we are now developing a 2-dimensional nonlinear code AEOLUS-P[6].

4. Low-n kink mode instability

A conducting wall surrounding the plasma is also effective to stabilize a low-n external kink mode instability. This was numerically confirmed by Berger et al. for the case of a tokamak with the Solov'ev equilibrium[7] and by Tsunematsu et al. for the case of a conventional circular cross-sectional tokamak with a more realistic current profile[8]. Both the calculations are carried out by using the code ERATO as in the previous section. According to the latter calculation the external n=1

mode instability is completely stabilized and the n=2 mode determines the beta limit if the position of the conducting wall Λ is less than about 1.2.

This result is obtained for the model equilibrium #1. Almost same result is obtained for the model equilibrium #2, i.e., a series of the FCT equilibria (Fig. 4.1)[1,9]. For this series of equilibria the n=1 kink mode is stabilized completely by a conducting wall at a practical position (Λ = 1.2). In order to stabilize the n=3 kink mode, the wall should be located more closely to the plasma surface but the position is still possible to realize. And for the higher beta plasma, the wall position should be more close. The difference of the critical wall position for the high and low beta plasmas, however, is slight among the instabilities with the same toroidal mode number. It is remarkable that the critical wall position is almost independent on the beta value. As the perturbations of higher mode number are localized near the plasma surface, the mode with n≥3 does not seem to be dangerous for the confinement (Fig. 4.2).

Generally the critical safety factor (q_{sc}) is increased by increasing the poloidal beta value. The total beta value, however, increases with the increase of β_p in the range of lower β_p. Therefore, the maximum attainable beta is determined by the tradeoff of how much β_p is gained against the loss of stability. The dependence of the beta value on the poloidal beta value is studied for the model equilibrium #1 of the INTOR plasma. In our analyses, we assume that a perfectly conducting wall is located at Λ=1.1. Therefore, it will be safe to say that the n=1 mode instability is strongly stabilized. It is also confirmed by the present analyses which show that the beta value is determined by the n=2 mode instabilities rather than the n=1 mode. By this analysis it is found that the stability sharply deteriorates in the parameter range of INTOR when the poloidal beta is increased (Fig. 4.3). In the higher β_p case of INTOR the instability of ballooning feature seems to determine the stability limit.

5. Low-n internal mode instability

From the viewpoint of beta optimization internal modes are very important. Numerical calculation of the low-n internal modes by ERATO is, however, rather difficult because of the small growth rates of the modes by comparing with the previously described external modes. Before obtaining definite conclusions on the behaviours of the modes from the results of the numerical calculations, therefore, it seems that we had better critically investigate the convergence properties of the numerical results and make some improvements on the code.[9,10,11)]

As a part of the investigation we calculated the growth rates for the n=3 internal modes for the model equilibrium #2 of INTOR. The results (Fig. 5.1) are consistent with those obtained by extrapolation from the higher-n results, which is described in the following section. The low-n internal modes for the lower beta equilibrium ($\beta \lesssim 10\%$) are marginally stable and those for higher beta equilibrium are slightly unstable.

6. High-n ballooning mode instability

Ballooning mode instabilities generally become more unstable as the toroidal mode number n becomes larger. Therefore, high-n ballooning mode instability is, usually, considered to be the most plausible cause which determines the limiting beta value of a present tokamak plasma. From this point of view we investigate the high-n ballooning mode instabilities in detail.

6.1 Numerical code BOREAS for the analysis of infinite-n ballooning modes[9,12)]

We develop a new high-n ballooning code BOREAS which solves the CHT (Connor, Hastie, and Taylor) equation[13)] on the basis of the finite element method. The equation which we solve is a one-dimensional eigenvalue equation defined on each magnetic surface of a tokamak,

$$\frac{\partial}{\partial s}\left\{\left[\frac{1}{R^2 B_\chi}+\frac{R^2 B_\chi^3}{B^2}Z^2\right]\frac{\partial F}{\partial s}\right\}+\frac{2P'}{B^2 B_\chi}\frac{\partial}{\partial \psi}\left(P+\frac{B^2}{2}\right)$$

$$-\frac{2P'I}{B^4}Z\frac{\partial}{\partial s}\left(\frac{B^2}{2}\right)\Big\}F+\omega^2\left[\frac{1}{R^2 B_\chi^3}+\frac{R^2 B_\chi}{B^2}Z^2\right]F=0,$$

5. Low-n internal mode instability

From the viewpoint of beta optimization internal modes are very important. Numerical calculation of the low-n internal modes by ERATO is, however, rather difficult because of the small growth rates of the modes by comparing with the previously described external modes. Before obtaining definite conclusions on the behaviours of the modes from the results of the numerical calculations, therefore, it seems that we had better critically investigate the convergence properties of the numerical results and make some improvements on the code.[9,10,11)]

As a part of the investigation we calculated the growth rates for the n=3 internal modes for the model equilibrium #2 of INTOR. The results (Fig. 5.1) are consistent with those obtained by extrapolation from the higher-n results, which is described in the following section. The low-n internal modes for the lower beta equilibrium ($\beta \lesssim 10\%$) are marginally stable and those for higher beta equilibrium are slightly unstable.

6. High-n ballooning mode instability

Ballooning mode instabilities generally become more unstable as the toroidal mode number n becomes larger. Therefore, high-n ballooning mode instability is, usually, considered to be the most plausible cause which determines the limiting beta value of a present tokamak plasma. From this point of view we investigate the high-n ballooning mode instabilities in detail.

6.1 Numerical code BOREAS for the analysis of infinite-n ballooning modes[9,12)]

We develop a new high-n ballooning code BOREAS which solves the CHT (Connor, Hastie, and Taylor) equation[13)] on the basis of the finite element method. The equation which we solve is a one-dimensional eigenvalue equation defined on each magnetic surface of a tokamak,

$$\frac{\partial}{\partial s}\left\{\left[\frac{1}{R^2 B_\chi}+\frac{R^2 B_\chi^3}{B^2}Z^2\right]\frac{\partial F}{\partial s}\right\}+\frac{2P'}{B^2 B_\chi}\frac{\partial}{\partial \psi}\left(P+\frac{B^2}{2}\right)$$

$$-\frac{2P'I}{B^4}Z\frac{\partial}{\partial s}\left(\frac{B^2}{2}\right)\Big\}F+\omega^2\left[\frac{1}{R^2 B_\chi^3}+\frac{R^2 B_\chi}{B^2}Z^2\right]F=0,$$

where

$$Z = \int_{y_o}^{y} \nu' dy ,$$

s is the arc length along the magnetic surface and the other notations are standard. From this lowest order equation a Lagrangian is reconstructed as

$$L = \int_{-\infty}^{\infty} [-B_1 (\frac{\partial F}{\partial s})^2 + P' \hat{B}_2 F^2 + \omega^2 B_3 F^2] ds,$$

where

$$B_1 = \frac{1}{R^2 B_\chi} + \frac{R^2 B_\chi^3}{B^2} Z^2 ,$$

$$B_2 = P'\hat{B}_2 = \frac{2P'}{B^2 B_\chi} \frac{\partial}{\partial \psi} (P + \frac{B^2}{2}) - \frac{2P'I}{B^4} Z \frac{\partial}{\partial s} (\frac{B^2}{2}) ,$$

$$B_3 = \frac{1}{R^2 B_\chi^3} + \frac{R^2 B_\chi}{B^2} Z^2 .$$

On the basis of the above Lagrangian the finite element formulation of the system is very easily derived and the problem is converted to a general eigenvalue problem of matrices.

The code BOREAS has two options. One solves the CHT equation directly as an eigenvalue problem of ω^2. The other calculates approximately the critical pressure gradient P' for the marginally stable equilibrium (ω^2=0). This solution is obtained by letting ω^2=0 and considering the equilibrium quantities are almost constant near the parameter range of interest.

Before using the code for the analyses of the INTOR plasma we apply the code for calculation of ballooning spectra of the Solov'ev equilibrium. Examples are shown in Figs. 6.1 and 6.2. In the respective order the subfigures a, b, and c correspond to the ballooning-and Mercier-stable equilibrium, ballooning-unstable but Mercier-stable equilibrium, and ballooning-and Mercier-unstable equilibrium. Several remarkable features are found in these figures. For example, number of unstable modes increases as the plasma becomes more unstable against the Mercier mode. Profiles of the eigenvectors show that unstable modes localize arround the center and, on the other hand, stable modes spread over the whole range of calculation. The most remarkable is found in the convergence curves of the eigenvalues (Fig. 6.2), which suggest that the positive spectra are continuous as the theory predicts. All these results seem very reasonable and the code BOREAS works well.

6.2 Dependence of the maximum beta on the poloidal beta

From the technological point of view it is one of the most important things to know the dependence of the maximum beta on the poloidal beta. For this purpose we calculated the maximum beta value obtained for the model equilibrium #1 and #2'.[2] The results (Fig. 6.3) are summarized as follows.

(1) The maximum attainable beta value depends strongly on the class of equilibria. Therefore, it is still possible to find out some new stable equilibria with higher beta value by adopting some special functional shape for the source term of the Grad-Shafranov equation.

(2) It seems that the maximum beta value is realized for relatively low poloidal beta equilibrium. This result is similar to that for the external kink mode. But variable range of classes of equilibria is limited and further studies are required to obtain a definite conclusion.

6.3 Ballooning-stable FCT equilibria and beta scaling

In order to obtain equilibria with high beta value for a given q-profile (model equilibrium #2) a 1-1/2 dimensional tokamak transport model[1,9,14] (APOLLO code) is applied to follow the evolution of tokamak equilibria subject to additional heating. Starting from a force-free equilibrium, we examine at every time step the stability condition for infinite-n ballooning modes (BOREAS code), and when they become unstable in some region the plasma transport is enhanced locally. We simply assume the infinite heat conduction due to the unstable modes which yields the marginally ballooning-stable pressure profile at each time step. We finally reach a high beta equilibrium marginally stable over the whole plasma column, in which the heating power balances the pressure transport due to the instabilities. To manifest the effects of ballooning modes on beta limitation, we ignore other dissipations in plasma transport and assume a temporally constant pressure source profile.

Now we describe the results of calculation for a class of plasma equiliblia with INTOR parameters, whose standard values are the aspect ratio A=4, ellipticity E=1.6, triangularity δ=0.3, safety factor at the magnetic axis and on the plasma surface q_0=1 and q_s=3, respectively. Figure 6.4 shows a typical time evolution of the pressure profile (Fig. 6.4a) and of the toroidal and poloidal beta values $\beta=2\mu_o\langle P\rangle/B_t^2$ and $\beta_J=4V\langle P\rangle/\mu_o R_o I_p^2$ (Fig. 6.4b). After the plasma becomes unstable at β=2.8%, the beta value continues to increase up to 4%, by changing the pressure

profile. We find that the slight reduction of the pressure gradient near the unstable region ensures the stability of ballooning modes, and the attainable beta value and the pressure profile are almost independent of the pressure source profile. In the calculation the external poloidal coil system is adjusted such that the plasma shape remains unchanged and no surface current appears. The finally established equilibrium configuration is shown in Fig. 6.4c.

From the systematic parameter survey according to the above procedure we obtain scaling laws of beta values on several parameters. Figure 6.5 summarizes the scaling laws, i.e., the attainable β and β_J, and also $\beta^* = 2\mu_o\sqrt{\langle P^2\rangle}/B_t^2$ as functions of E, δ, q_s and A. Higher β values can be reached as expected with increasing E and/or decreasing A and q_s, while the effect of δ is found to be insignificant. It should be noted that these scaling laws are for the series of the FCT equilibria (model equilibrium #2).

6.4 Finite-n correction and kinetic effect on the high-n ballooning modes

The beta limit obtained from the infinite-n ballooning mode analysis in the previous subsection is too restrictive. It has been shown that the growth rate of these modes are reduced by decreasing n[13,15]. Another stabilization is expected from kinetic effects. The FLR effect stabilizes high-n MHD modes, and can be included in the MHD eigenmode equation simply by replacing ω^2 to $\omega(\omega+\omega_{*i})$, where ω_{*i} is the ion diamagnetic drift frequency[1,16]. Taking account of these effects, we can formally write the growth rate in the form $\gamma^2(n) = \gamma_\infty^2 - \gamma_{fn}^2 - \omega_{*1}^2/4$ (γ_∞:the growth rate for $n\to\infty$, the second and third terms correspond to the stabilization due to the finite-n correction and FLR, respectively). Note that this formula can determine the n value and the corresponding growth rate for the most unstable mode because γ_{fn}^2 scales as n^{-1}, while $\omega_*^2/4 \propto n^2$.

We calculate $\gamma^2(n)$ for standard parameters in the previous subsection under the plasma heating with rather broad source profile $S \propto (1-\psi)^{1.5}$. In Fig. 6.6a, the dashed line denotes the MHD growth rate, $\gamma_\infty^2 - \gamma_{fn}^2$, derived by WKB method[15], and the solid curve the growth rate including ω_* effect, $\gamma^2(n)$, for the temperature T_i=20 keV. The critical n is about 20 and the corresponding growth rate is $\gamma^2 \simeq 0.06\ \omega_A^2$ ($\omega_A^2 = B^2/\mu_o\rho R_o^2$). In this figure, the dotted line denotes the CHT theory[13], and it is completely stabilized by ω_* effects. Figure 6.6b shows the γ-n-β diagram; we can

see that the critical beta value is larger than the one predicted by the infinite-n calculations and that the maximum growth rate starts to decrease for the beta value 12%. This result suggests that if we carefully control the plasma shape and the pressure profile, we can reach higher beta value, although the critical beta is rather small in the present case. Moreover, the self-healing effect of the pressure profile due to unstable modes, as described in the previous subsection, must be included in order to determine the critical beta value.

6.5 Possibility to attain higher beta equilibrium in second stable region

Existence of the second stable region was pointed out theoretically since the early stage of the high-n ballooning mode analyses[17]. The theory predicts that a plasma on an unstable magnetic surface will become again stable when the pressure gradient on the surface is further increased beyond a certain critical value. However, an equilibrium in the second stable region over the whole plasma cross-section has not been found up to now. Therefore, it is not evident if a simple procedure to get over the ballooning-unstable band will be always found for any kind of initial equilibrium. We find out an example of the procedure by which a high beta equilibrium stable against the ballooning mode in a whole plasma region is obtained[18] (Fig.6.7).

The procedure is based on the combination of the APOLLO and BOREAS codes as in subsection 6.3. We start from the force-free equilibrium with circular cross-section and heat up the plasma with constant source profile $S(\psi) = (1-\psi^2)^2$. When the plasma is heated up to $\beta \simeq 2\%$, it becomes unstable at the region where the pressure gradient is maximum. But the heating is continued beyond this beta value. During the process the unstable region spreads in both directions and finally the second stable region appears in the midway of the unstable region. Then we introduce the stabilization transport process as described in subsection 6.3 and whole plasma is made stable. Figure 6.7 shows the example of the equilibrium with $\beta \simeq 15\%$ which is stable against the ballooning mode in a whole plasma region. In this figure $\left|\left(\frac{dP}{d\psi}\right)_{crit}\right|$ is the critical pressure gradient for the ballooning mode and $\left|\left(\frac{dP}{d\psi}\right)_{crit}\right| \geq \left|\frac{dP}{d\psi}\right|$ ensures the ballooning mode is marginally stable. In this stabilization transport process the pressure profile changes only slightly and the beta value changes very slightly. Thus a ballooning-stable equilibrium with very high beta value is attained

by this procedure.

In an experiment of an actual plasma more realistic method to get over the ballooning unstable band should be adopted, though the simplest may be to heat up the plasma very quickly. The example shown in Fig. 6.7 is for a circular cross-sectional tokamak and the result is not directly applied to the INTOR plasma. But we consider that the above procedure will be also successful for the INTOR plasma and it is now in progress.

7. Resistive instability

7.1 Kinetic theory of a tearing mode instability[19,20]

As the temperature becomes high enough, the growth rate of the resistive tearing mode, γ_T, becomes smaller than the drift frequency ω_*. For plasma parameters of INTOR such as B=5.5T, a=1.3m, R=5.2m, $n_0=10^{14}cm^{-3}$, T_e=10keV and (m,n) = (2,1), i.e., $S\sim10^{10}$ (S: resistive skin time / Alfvén time), the growth rate obtained from the fluid theory is of the order of $10^{-3}\omega_*$. The stability is dominated by the kinetic interactions near the mode rational surface.

We have developed a unified theory of the low frequency modes in a circular cylindrical tokamak: the density inhomogeneity, plasma current, β value, q-profile, magnetic shear, finite gyroradius, electron temperature gradient and kinetic parallel conductivity effects are correctly taken into account. The stability is examined in the collisionless limit. We find that the low m (m = 2.3, ...) drift tearing instabilities can appear in low density regime and are stabilized due to ion Landau damping when the density increases. These are further stabilized by increasing the electron temperature gradient.

Numerical calculations are performed for model distribution of the equilibrium as $N(r) = n(0)\exp(-r^2/2L_n^2)$, $J_0(r) = J_0\exp(-\eta_J r^2/2L_n^2)$, $T_e(r)= T_0\exp(-\eta_e r^2/L_n^2)$. We take the density inhomogeneity scale length L_n equal to a/2; in this case the line averaged density $\bar{N}(r) = n(0)/2$ holds. Further choice of the parameters are B = 4T, a = 50cm, R = 2m, $T_e(0)$ = 4keV and T_i = 2kev. For these parameters $a/\rho_i \sim 500$ holds.

The figure 7.1 shows the eigenvalue ω of the (2,1) mode as a function of the density n(0) for the parameters q(0) = 1.49, q(a) = 3.43, η_J = 1 and $\Delta'a$ = 12.1 (unstable region for MHD tearing mode). When the plasma density is low, the (2,1) mode is unstable with the growth rate of the order $0.1\omega_*$; as the density increases γ reduces and the drift-tearing mode

by this procedure.

In an experiment of an actual plasma more realistic method to get over the ballooning unstable band should be adopted, though the simplest may be to heat up the plasma very quickly. The example shown in Fig. 6.7 is for a circular cross-sectional tokamak and the result is not directly applied to the INTOR plasma. But we consider that the above procedure will be also successful for the INTOR plasma and it is now in progress.

7. Resistive instability

7.1 Kinetic theory of a tearing mode instability[19,20)]

As the temperature becomes high enough, the growth rate of the resistive tearing mode, γ_T, becomes smaller than the drift frequency ω_*. For plasma parameters of INTOR such as B=5.5T, a=1.3m, R=5.2m, $n_0=10^{14}cm^{-3}$, T_e=10keV and (m,n) = (2,1), i.e., $S\sim10^{10}$ (S: resistive skin time / Alfvén time), the growth rate obtained from the fluid theory is of the order of $10^{-3}\omega_*$. The stability is dominated by the kinetic interactions near the mode rational surface.

We have developed a unified theory of the low frequency modes in a circular cylindrical tokamak: the density inhomogeneity, plasma current, β value, q-profile, magnetic shear, finite gyroradius, electron temperature gradient and kinetic parallel conductivity effects are correctly taken into account. The stability is examined in the collisionless limit. We find that the low m (m = 2.3, ...) drift tearing instabilities can appear in low density regime and are stabilized due to ion Landau damping when the density increases. These are further stabilized by increasing the electron temperature gradient.

Numerical calculations are performed for model distribution of the equilibrium as $N(r) = n(0)\exp(-r^2/2L_n^2)$, $J_0(r) = J_0\exp(-\eta_J r^2/2L_n^2)$, $T_e(r)= T_0\exp(-\eta_e r^2/L_n^2)$. We take the density inhomogeneity scale length L_n equal to a/2; in this case the line averaged density $\bar{N}(r) = n(0)/2$ holds. Further choice of the parameters are B = 4T, a = 50cm, R = 2m, $T_e(0)$ = 4keV and T_i = 2kev. For these parameters $a/\rho_i \sim 500$ holds.

The figure 7.1 shows the eigenvalue ω of the (2,1) mode as a function of the density n(0) for the parameters q(0) = 1.49, q(a) = 3.43, η_J = 1 and $\Delta'a$ = 12.1 (unstable region for MHD tearing mode). When the plasma density is low, the (2,1) mode is unstable with the growth rate of the order $0.1\omega_*$; as the density increases γ reduces and the drift-tearing mode

finally is stabilized for $n(0) \geq 7\times10^{13}cm^{-3}$. The judgement of the stability in terms of a simple Δ' analyses, $\Delta' \gtrless 0$, is no longer valid for collisionless kinetic tearing mode.

The wave structure implies that the stability is determined by the balance between excitations by electrons and the convective loss. The stability criterion of (2,1) mode is shown in Fig. 7.2 for $T_e = T_i$ and $T_e = 2T_i$ and other parameters are the same as Fig. 7.1. The stability condition is approximately obtained as

$$u/v_i \lesssim 0.4,$$

for the present parameters (J_0 = -Neu). We see that the local current density, not Δ', is crucial to excite the drift tearing instability. The value 0.4 itself should depend on the equilibrium configurations (q, η_J, ...), but the dependence is not investigated here. The figure 7.3 shows γ/ω_* as a function of T_i for $n(0) = 10^{14}cm^{-3}$. The solid line is due to the theory where the electron-ion collisions are taken into account. This shows the relation of the kinetic tearing mode to the resistive tearing mode.

In summary, for the high temperature plasmas, all electromagnetic helical modes ($2 \leq m \lesssim 50$), which have the mode rational surface in the hot core of the plasma, are stable in the high density cylindrical tokamak equilibria with the moderate current and temperature inhomogeneities $\eta_J \sim \eta_e \sim 1 - 2$. When the mode rational surface is near the plasma edge, T (rational surface) $\lesssim$ O(100)eV, MHD tearing mode can be unstable if $\Delta' > 0$ is satisfied.

Our analyses shows the importance of the energy convection as the stabilization mechanism. This implies that the toroidal effect[21] and the steep ion temperature gradient[22] remains to be possible candidates as the cause of destabilization of kinetic tearing mode.

The growth of the (2,1) tearing mode is believed to lead the onset of the major disruption; the stabilization of the tearing mode due to the kinetic interactions suggests that the occurance of the major disruption becomes less frequent in high temperature plasmas. These problems and also the study of m = 1 drift tearing mode remain open and still require further investigations.

7.2 Saturation of the m=1 magnetic island due to a resistive internal mode

When the safety factor at the magnetic axis becomes below the unity, the internal disruption (or the sawtooth oscillation) is observed in a tokamak[23], and this phenomenon is well explained by the m=1 resistive mode, which was proposed by Kadomtsev[24] and confirmed numerically by other authors[25,26]. The recent high power neutral beam injection experiments of the JFT-2 tokamak[27], however, showed the suppression of the internal disruption and the appearance of the m=1 stationary oscillation with large amplitude. One of the possible explanations of this new phenomenon is the stability of the m=1 internal mode. As was predicted by Bussac et al.[28], the internal mode becomes unstable in a toroidal plasma, when the poloidal beta value exceeds a certain critical value. Although the saturation level of this mode is quite low due to the development of the skin current at the q=1 surface, as pointed out by Rosenbluth et al.[29], the finite resistivity η can relax this skin current and cause the large magnetic island. From this point of view, we studied the linear stability and nonlinear evolution of the resistive internal mode[30].

The nonlinear evolution of the resistive modes in a tokamak has been studied by using the reduced set of MHD equations[26]. But this set of equations cannot express the unstable m=1 internal mode because of neglecting the second order terms of the inverse aspect ratio. Therefore, we developed the new reduced set of MHD equations in a cylindrical plasma under the assumption of the incompressible fluid motion $\nabla\cdot\vec{v} = 0$. This new set of equations is reduced to the conventional one when the longitudinal wave number k_z goes to infinity with keeping $k_z B_z$ constant. This set of equations has been solved by expanding variables into Fourier components and using the predictor-corrector explicit time integration scheme. Figure 7.4 shows the temporal change of the position of the magnetic axis r_a due to the resistive mode, the resistive internal mode, and the internal mode. The safety factor and the pressure profile are chosen as $q(r) = 0.8(1+r^2)$ and $p(r) = 2(1-r^2)$, respectively, and the magnetic fields B_θ and B_z are given by solving the equilibrium equation under the condition of $B_\theta = 1$ at $r=0.5$. When $k_z = 0$ and $\eta=10^{-4}$, the internal mode is marginally stable and the magnetic axis shifts to the cooler region exponentially in time due to the resistive mode, and the internal disruption occurs when the magnetic axis touched the critical surface $r = r_c$, as predicted by Kadomtsev. When $k_z = 1/3$ and $\eta= 0$, the

internal mode shifts the magnetic axis, but this shift saturates at low level, which is consistent with the analysis by Rosenbluth et al. When we take into account the finite resistivity $\eta = 10^{-4}$, then the magnetic axis shifts beyond this level due to the magnetic island formation, as the resistive mode, but the shift saturates before touching the critical surface. This saturation of the magnetic shift is caused by the island formation of the B_z field, which is constant in time for the resistive mode. Figure 7.5 shows the magnetic flux surface at the saturation level.

In this simulation, we have shown that the internal disruption can be suppressed in a tokamak with low q value and high poloidal beta value. As was pointed out in DIVA experiments[31], the internal disruption decreases the energy confinement time considerably in a low q discharge. Therefore, the suppression of the internal disruption will improve the energy confinement. The results of the simulations will be reported in detail elsewhere.

8. Conclusions

Results of the analyses are summarized as follows.

Positional instability of the INTOR plasma is stabilized by a conducting wall located at $\Lambda \leq 1.5$. In the present design of INTOR the positional instability does not seem to limit the maximum attainable beta but if higher ellipticity is adopted the situation changes to be more restrictive.

Low-n kink instability is stabilized by a conducting wall located at technologically possible position ($\Lambda \simeq 1.1$). Higher-n kink instability seems to be safe by judging from the radial mode structure. In this sense it seems that there is no serious beta limitation due to the mode.

Low-n internal mode instability is well understood as the extrapolation from the higher-n ballooning mode instabilities and, generally, the low-n mode has smaller growth rate than the higher-n modes.

As for the high-n ballooning mode instabilities there are many points to be mentioned.

(1) Higher beta equilibrium which is stable against the high-n ballooning mode is obtained by incorporating the stabilization-transport process to the 1-1/2 dimensional tokamak code (equilibrium-transport code). In this procedure of optimization the q-profile is not altered and usually the gain of beta value due to the process is not very large.

internal mode shifts the magnetic axis, but this shift saturates at low level, which is consistent with the analysis by Rosenbluth et al. When we take into account the finite resistivity $\eta = 10^{-4}$, then the magnetic axis shifts beyond this level due to the magnetic island formation, as the resistive mode, but the shift saturates before touching the critical surface. This saturation of the magnetic shift is caused by the island formation of the B_z field, which is constant in time for the resistive mode. Figure 7.5 shows the magnetic flux surface at the saturation level.

In this simulation, we have shown that the internal disruption can be suppressed in a tokamak with low q value and high poloidal beta value. As was pointed out in DIVA experiments[31], the internal disruption decreases the energy confinement time considerably in a low q discharge. Therefore, the suppression of the internal disruption will improve the energy confinement. The results of the simulations will be reported in detail elsewhere.

8. Conclusions

Results of the analyses are summarized as follows.

Positional instability of the INTOR plasma is stabilized by a conducting wall located at $\Lambda \leq 1.5$. In the present design of INTOR the positional instability does not seem to limit the maximum attainable beta but if higher ellipticity is adopted the situation changes to be more restrictive.

Low-n kink instability is stabilized by a conducting wall located at technologically possible position ($\Lambda \simeq 1.1$). Higher-n kink instability seems to be safe by judging from the radial mode structure. In this sense it seems that there is no serious beta limitation due to the mode.

Low-n internal mode instability is well understood as the extrapolation from the higher-n ballooning mode instabilities and, generally, the low-n mode has smaller growth rate than the higher-n modes.

As for the high-n ballooning mode instabilities there are many points to be mentioned.

(1) Higher beta equilibrium which is stable against the high-n ballooning mode is obtained by incorporating the stabilization-transport process to the 1-1/2 dimensional tokamak code (equilibrium-transport code). In this procedure of optimization the q-profile is not altered and usually the gain of beta value due to the process is not very large.

(2) The scaling laws of the optimized beta value are obtained. The remarkable is the $1/\sqrt{q_s}$ - scaling of the beta value which is different from the usually obtained $1/q_s^2$-scaling. Studies of scaling laws on other parameters are now being carried out.

(3) It is quantitatively shown that the combination of finite-n correction and kinetic effect stabilizes the ballooning mode instability considerably. More systematic parameter survey is now planned.

(4) An example of a very high beta equilibrium in the second stable region of the ballooning mode instability is obtained successfully.

Kinetic approach of the tearing mode instability shows that the usual MHD approach is not always appropriate in the case of a high temperature plasma. In the case difference of stability criterion between the two approaches seems rather serious. More detailed studies are needed on this problem.

In order to understand many nonlinear MHD phenomena which include major disruption and large-scale oscillations in a tokamak plasma several time-evolutional codes are being developed. As an example of the analyses a resistive internal mode instability is successfully analyzed to interprete a large amplitude stationary oscillation observed in the JFT-2 experiment by a large-scale island formation. This kind of analysis on the INTOR plasma is not completed yet.

Acknowledgments

The authors would like to thank Dr. M. Tanaka for his helpful discussion and continuing encouragement. It is our great pleasure to express our sincere thanks to Dr. Y. Obata for his encouragement throughout the whole work.

(2) The scaling laws of the optimized beta value are obtained. The remarkable is the $1/\sqrt{q_s}$ - scaling of the beta value which is different from the usually obtained $1/q_s^2$-scaling. Studies of scaling laws on other parameters are now being carried out.

(3) It is quantitatively shown that the combination of finite-n correction and kinetic effect stabilizes the ballooning mode instability considerably. More systematic parameter survey is now planned.

(4) An example of a very high beta equilibrium in the second stable region of the ballooning mode instability is obtained successfully.

Kinetic approach of the tearing mode instability shows that the usual MHD approach is not always appropriate in the case of a high temperature plasma. In the case difference of stability criterion between the two approaches seems rather serious. More detailed studies are needed on this problem.

In order to understand many nonlinear MHD phenomena which include major disruption and large-scale oscillations in a tokamak plasma several time-evolutional codes are being developed. As an example of the analyses a resistive internal mode instability is successfully analyzed to interprete a large amplitude stationary oscillation observed in the JFT-2 experiment by a large-scale island formation. This kind of analysis on the INTOR plasma is not completed yet.

Acknowledgments

The authors would like to thank Dr. M. Tanaka for his helpful discussion and continuing encouragement. It is our great pleasure to express our sincere thanks to Dr. Y. Obata for his encouragement throughout the whole work.

References

1) M. Azumi et al., "Envolution of Stable High Beta Tokamak Equilibria", 8th Int. Conf. on Plasma Physics and Controlled Nuclear Fusion Research, Brussels, 1980, IAEA-CN-38/K-1-1.
2) T. Takeda et al., "IAEA INTOR Workshop Report —— Stability Control ——", JAERI-M 8624 (1980).
3) D. Berger et al., "A Two Dimensional MHD Stability Code with a Finite Hybrid Expansion in Both Directions", 2nd European Conf. on Computational Physics, Garching, 1976 IPP 6/147 C3.
4) L.C. Bernard et al., "Stabilization of Ideal MHD Modes", GA-A15236 (1979).
5) G. Laval et al., Phys. Fluids 17 (1974) 835.
6) G. Kurita et al., "Nonlinear Stability Analysis of Axisymmetric Instabilities", to be published in JAERI-M.
7) D. Berger et al., "Wall Stabilization Action of MHD Instabilities", ORNL/TM-6219 (1978).
8) T. Tsunematsu et al., "Beta Limit of a Large Tokamak with a Circular Cross-Section", to be published in JAERI-M.
9) T. Takizuka et al., "Computational Studies of Tokamak Plasmas", JAERI-M 9354 (1981).
10) T. Tsunematsu et al., Comput. Phys. Commun. 19 (1980) 179.
11) T. Takizuka et al., "Effects of the Finite Hybrid Element on MHD Stability Calculations in a Cylindrical Plasma", to be published in Comput. Phys. Commun.
12) M. Azumi et al., "A Finite Element Approach to the High-n Ballooning Mode Stability Analysis", to be submitted to Comput. Phys. Commun.
13) J.W. Connor et al., Proc. Phys. Soc. A365 (1979) 1.
14) M. Azumi et al., "Axisymmetric Toroidal Equilibrium Code SELENE40 for 2D Tokamak Transport Simulation", to be published in JAERI-M.
15) R.L. Dewar et al., "WKB Theory for High-n Modes in Axisymmetric Toroidal Plasma", PPPL-1587 (1979).
16) K. Itoh et al., J. Phys. Soc. Japan 50 (1981) 660.
17) B. Coppi et al., Nucl. Fusion 19 (1979) 715.
18) M. Azumi et al., "High Beta Tokamak Equilibrium in the Second Stable Region", to be submitted to J. Phys. Soc. Japan.
19) S.I. Itoh and K. Itoh, Nucl. Fusion 21 (1981) 3.
20) K. Itoh and S.I. Itoh, Phys. Letters 82 (1981) 85.

21) K. Itoh et al., J. Phys. Soc. Japan 50 (1981) 635.
22) S. Inoue et al., Nucl. Fusion 18 (1978) 755.
23) S. von Goeler et al., Phys. Rev. Letters 33 (1974) 1201.
24) B.B. Kadomtsev, Fizika Plasmy 1 (1975) 710.
25) A. Sykes and Wesson, Phys. Rev. Letters 37 (1976) 140.
26) B.V. Waddel et al., Nucl. Fusion 16 (1976) 528.
27) S. Yamamoto et al., "Magnetohydrodynamic Activities in JFT-2 Tokamak with High Power Neutral Beam Injection Heating", submitted to Nucl. Fusion.
28) M.N. Bussac et al., Phys. Rev. Letters 35 (1975) 1638.
29) M.N. Rosenbluth et al., Phys. Fluids 16 (1973) 1894.
30) B. Coppi et al., "Resistive Internal Kink Modes", MATT-1271 (1976).
31) DIVA group, Nucl. Fusion 20 (1980) 271.

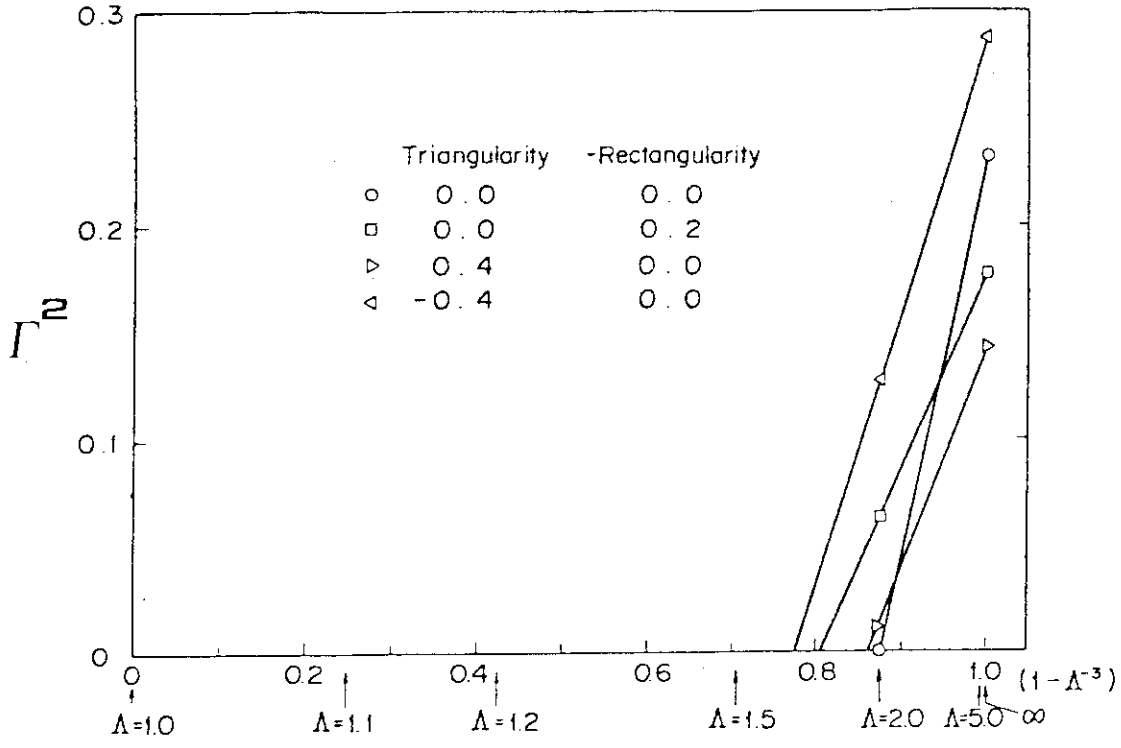

Fig. 3.1 Square of growth rate (Γ^2) of positional instability versus the position of a conducting wall, where q_a=2.5, β_p=1.3, and E=1.5.

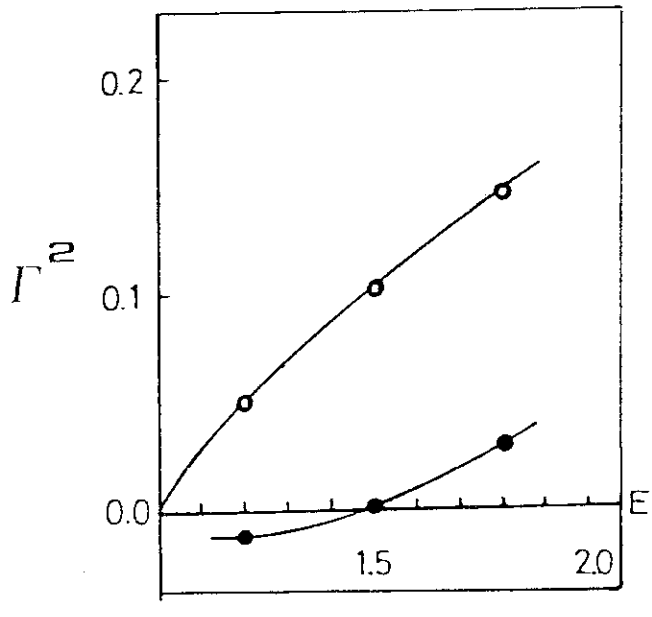

Fig. 3.2 Square of growth rate (Γ^2) of positional instability versus ellipticity E for Λ = 1.6 (●) and ∞(o), where q_a=4.0 and β_p=2.0.

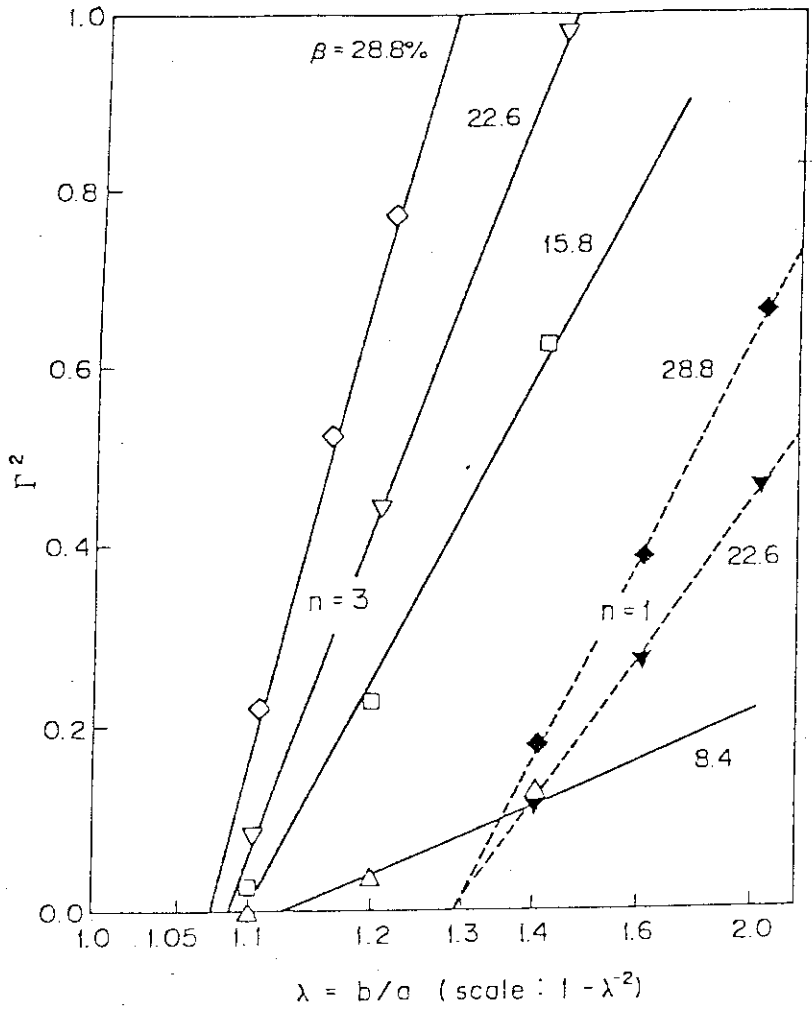

Fig. 4.1 Square of growth rate (Γ^2) of kink instability versus the position of a conducting wall (Λ=b/a) for a series of FCT equilibria. Symbols Δ, $\square$, ∇, and $\diamond$ denote the cases with β=8.4, 15.8, 22.6. and 28.8% for n=1 (black symbol) and n=3 (open symbol) modes, respectively.

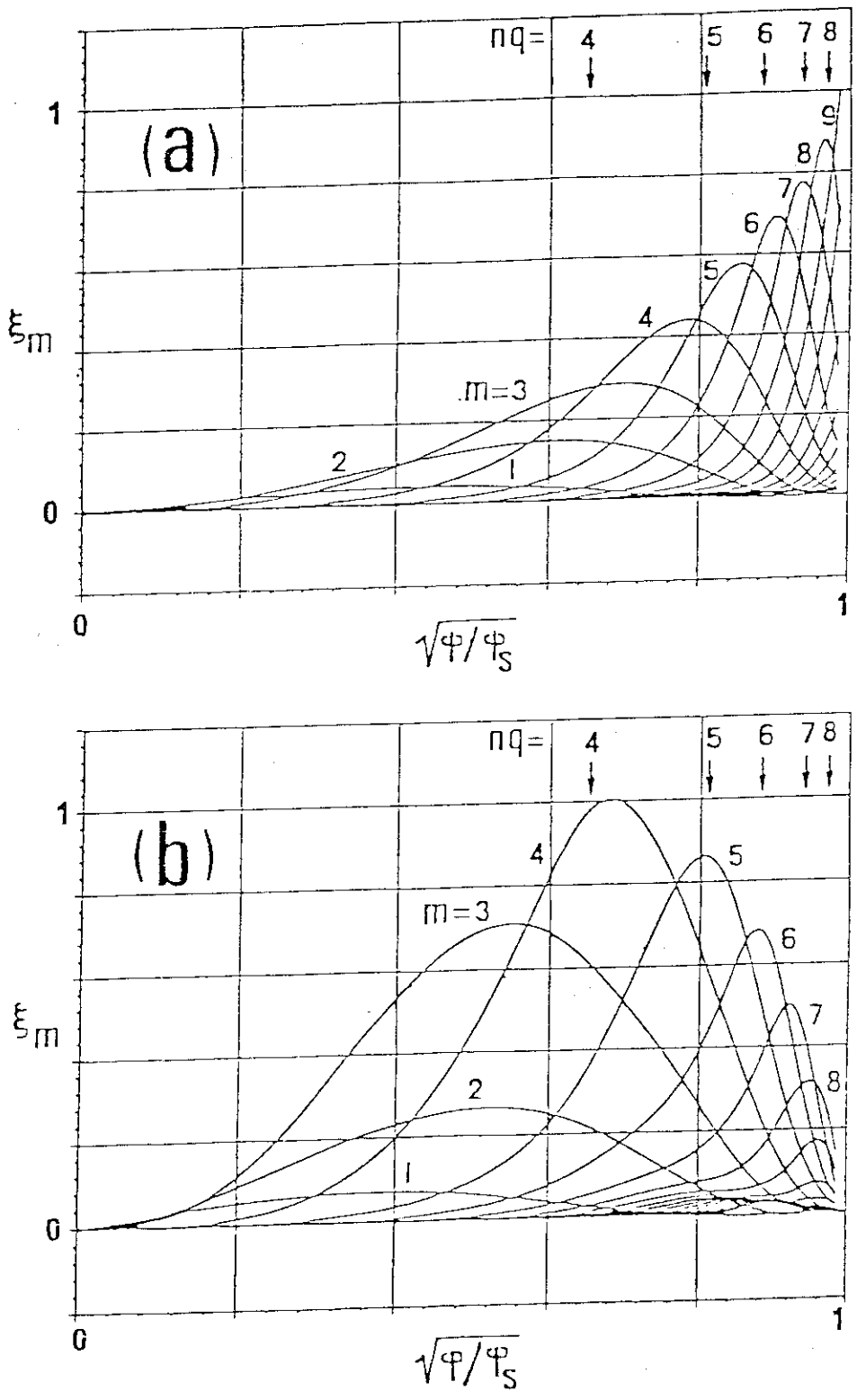

Fig. 4.2 Fourier decomposed displacements $\xi_\psi(\sqrt{\psi})$ for the case of n=3 kink mode (Λ=1.1, Fig.4.2a) and internal mode (Fig. 4.2b) of the equilibrium with β=22.6%.

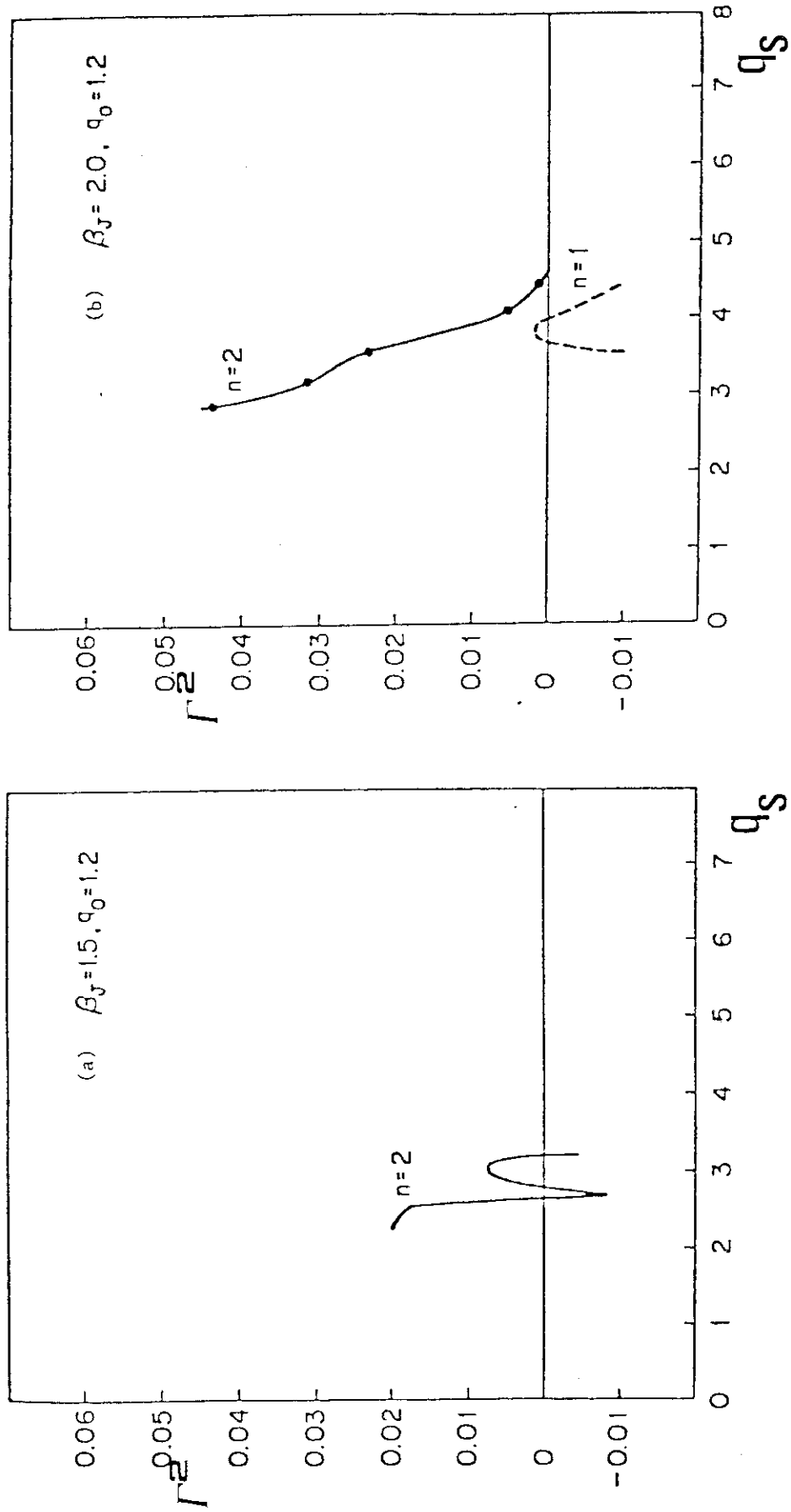

Fig. 4.3 Square of growth rate versus the safety factor at the plasma boundary (q_s) for the model equilibrium #1. (a) β_J=1.5 and (b) β_J=2.0.

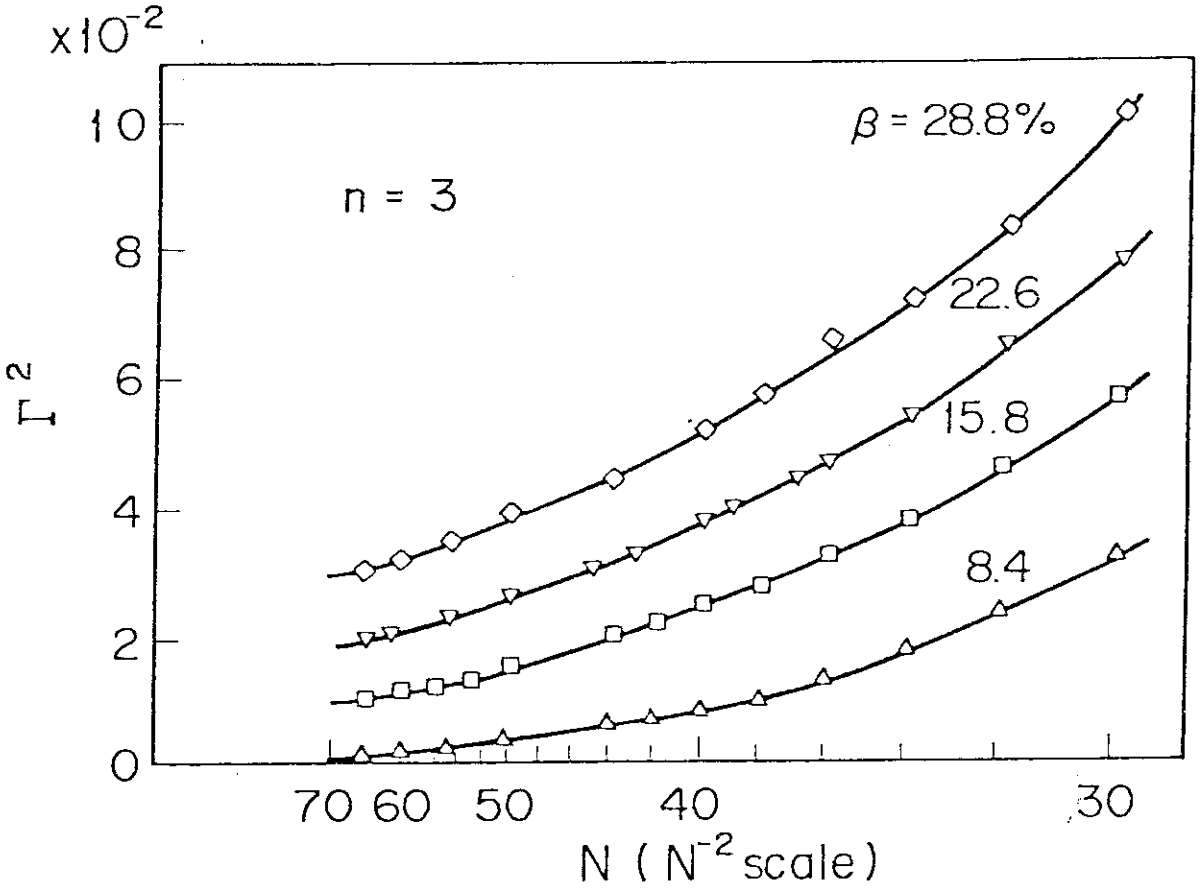

Fig. 5.1 Convergence curves of Γ^2 vs. N^{-2} ($N = N_\psi = N_\chi$ is the number of meshes) for the n=3 internal modes.

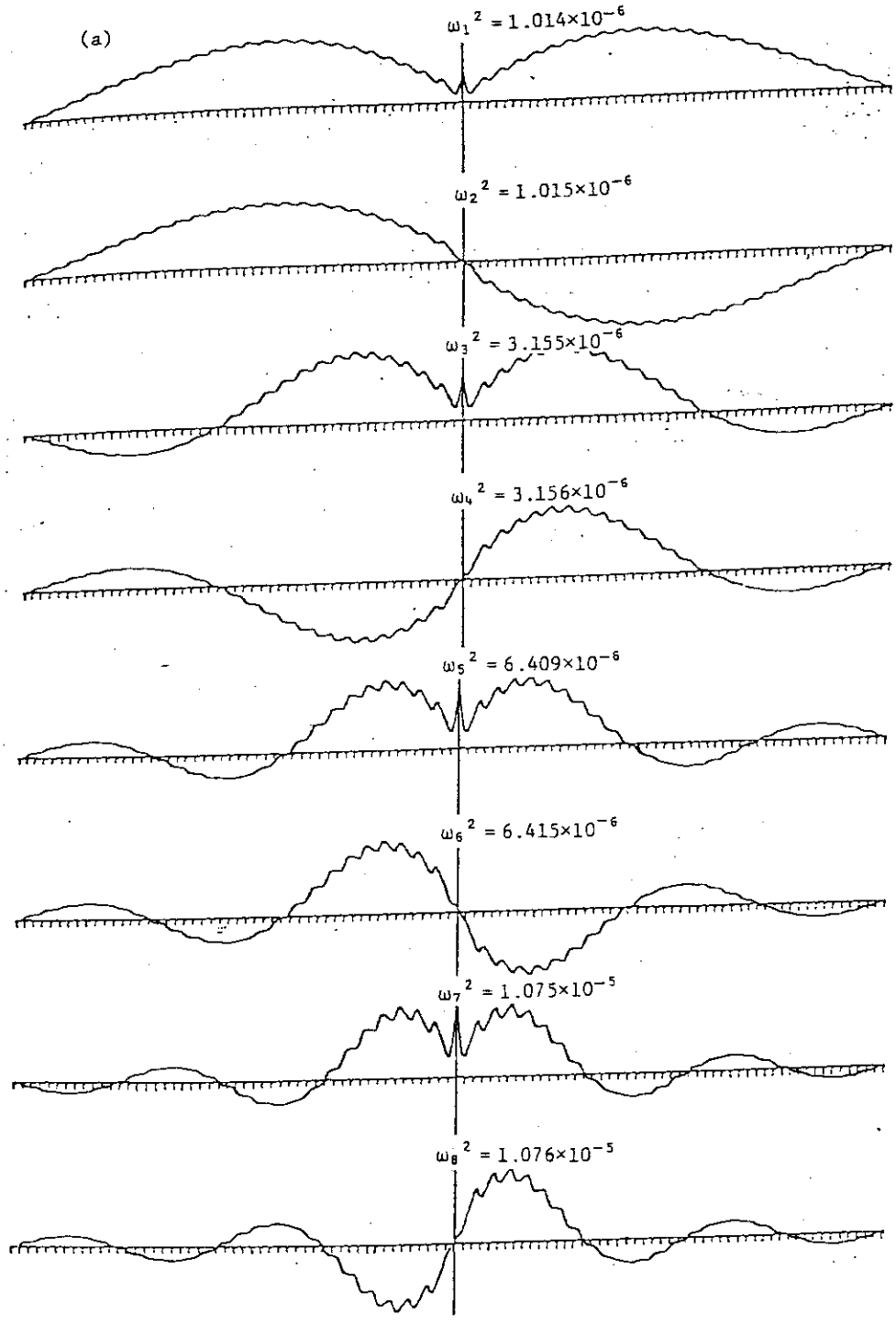

Fig. 6.1 Eigenvalues (ω^2) and eigenfunctions of the infinite-n modes on a magnetic surface ψ/ψ_s=0.5. An equilibrium is of the Solov'ev type with A=3. Solutions are obtained by using the integration boundary θ_{max}=50π. (a) q_0=1.5, where both the Mercier- and ballooning-modes are stable.

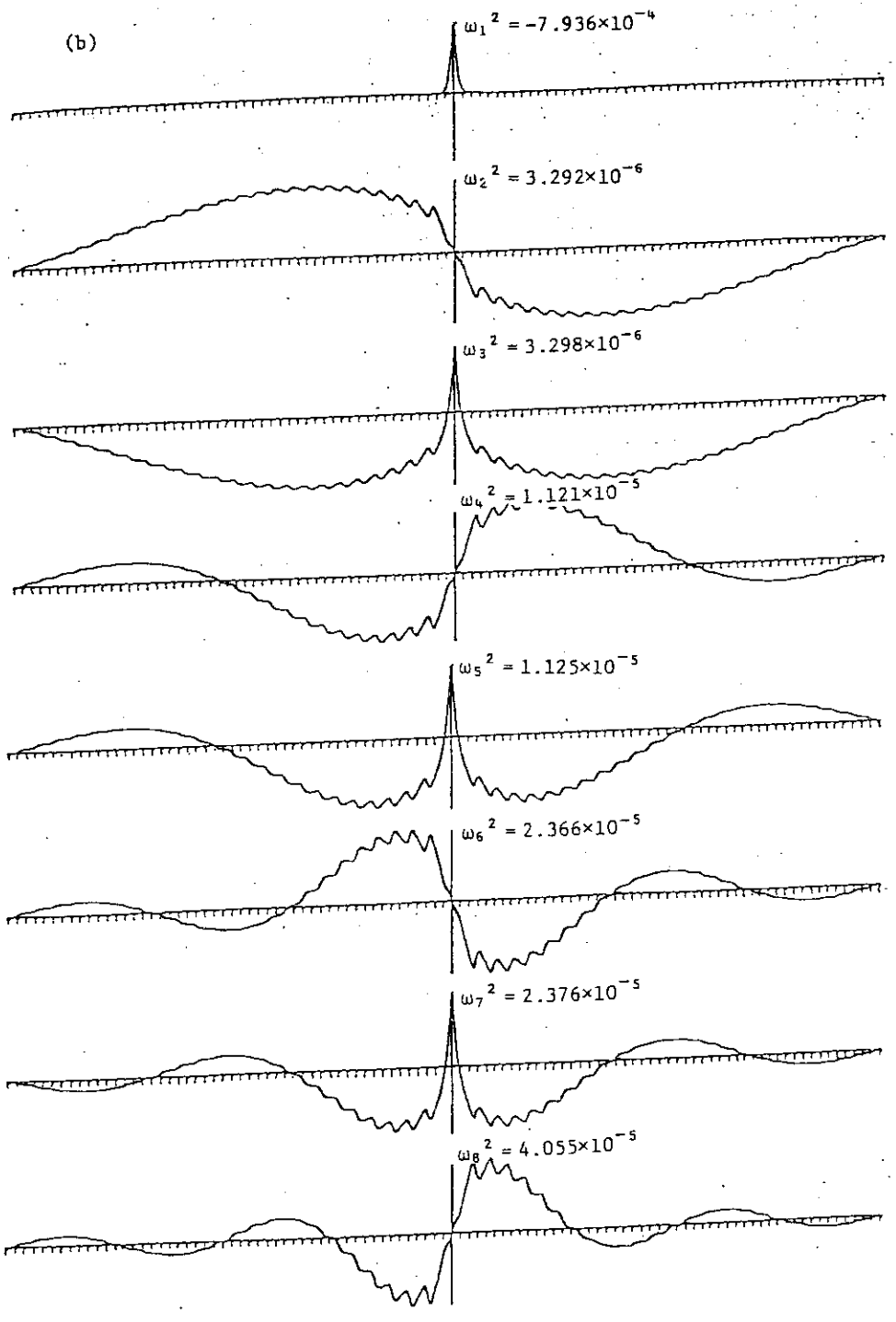

Fig. 6.1 Eigenvalues (ω^2) and eigenfunctions of the infinite-n modes on a magnetic surface ψ/ψ_s=0.5. An equilibrium is of the Solov'ev type with A=3. Solutions are obtained by using the integration boundary $\theta_{max}=50\pi$. (b) q_0=1.0, where the Mercier-mode is stable. The lowest eigenvalue becomes negative and corresponding eigenfunction is strongly localized near θ=0.

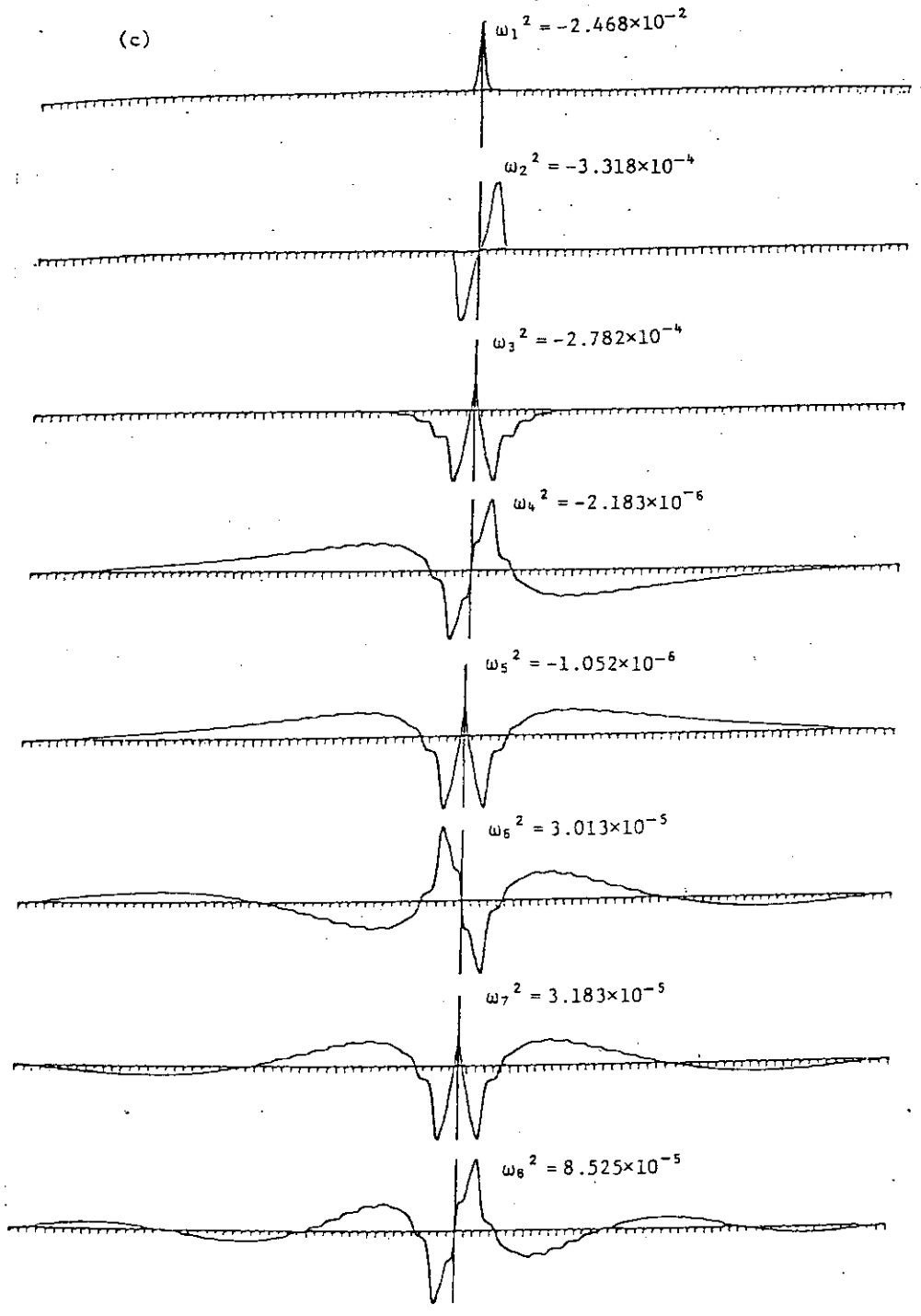

Fig. 6.1 Eigenvalues (ω^2) and eigenfunctions of the infinite-n modes on a magnetic surface ψ/ψ_s=0.5. An equilibrium is of the Solov'ev type with A=3. Solutions are obtained by using the integration boundary θ_{max}=50π. (c) q_0=0.5, where the Mercier-mode is unstable.

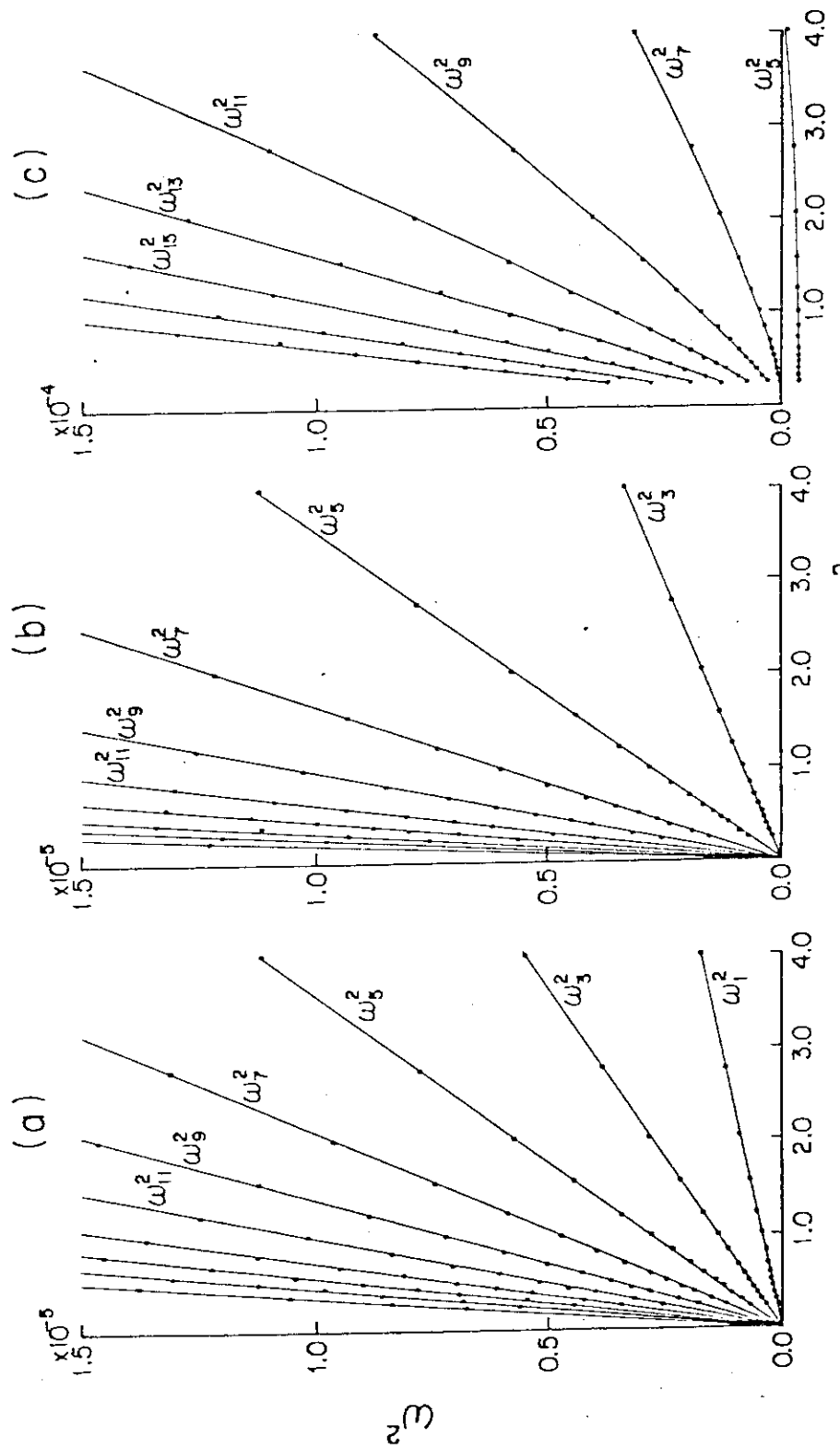

Fig. 6.2 Convergence curves of ω^2 versus θ_{max}^{-2} for the cases (a) q_0=1.5, (b) q_0=1.0, and (c) q_0=0.5. In (a) and (b) positive eigenvalues ω^2 are proportional to θ_{max}^{-2}, while the convergence property in (c) is much different from that in (a) and (b).

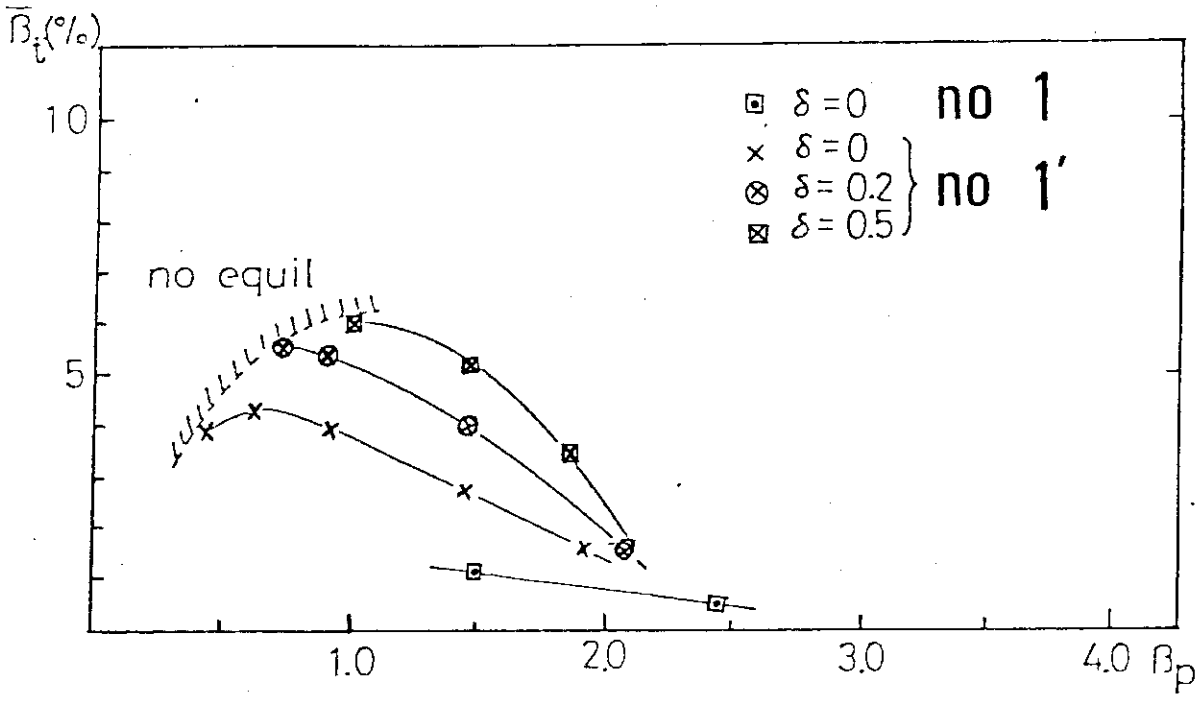

Fig. 6.3 The critical beta value due to the high-n balloning mode versus the poloidal beta value.

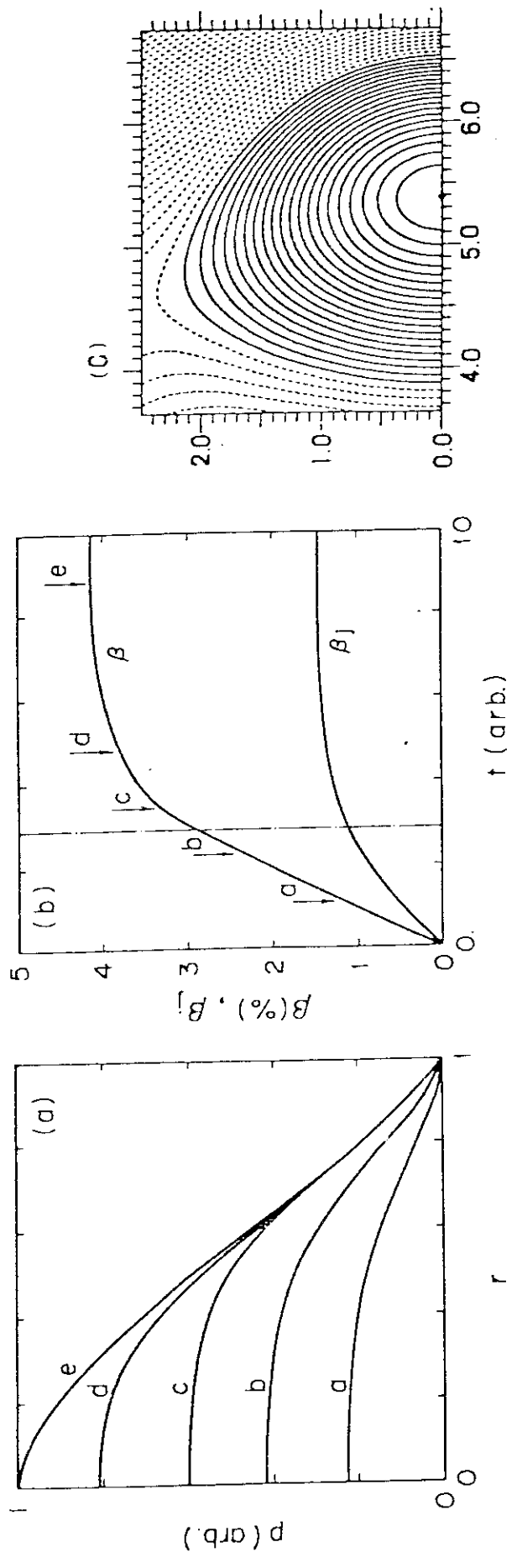

Fig. 6.4 Evolution of (a) the pressure profile and (b) the toroidal and poloidal beta values of a plasma with INTOR parameters: A=4, E=1.6, δ=0.3, q_0=1, and q_3=3. The pressure source profile $S\propto(1-\psi)^2$ is assumed. The marginally stable plasma with β=4.2% is realized after the ballooning modes become unstable at β=2.8% (the dotted solid line in (b)). The minor radius r in (a) is defined by $r=\sqrt{\phi/\phi_s}$ where ϕ is the toroidal flux and the suffix s corresponds to the value on the plasma surface. (c) The final equilibrium configuration with β=4.2%.

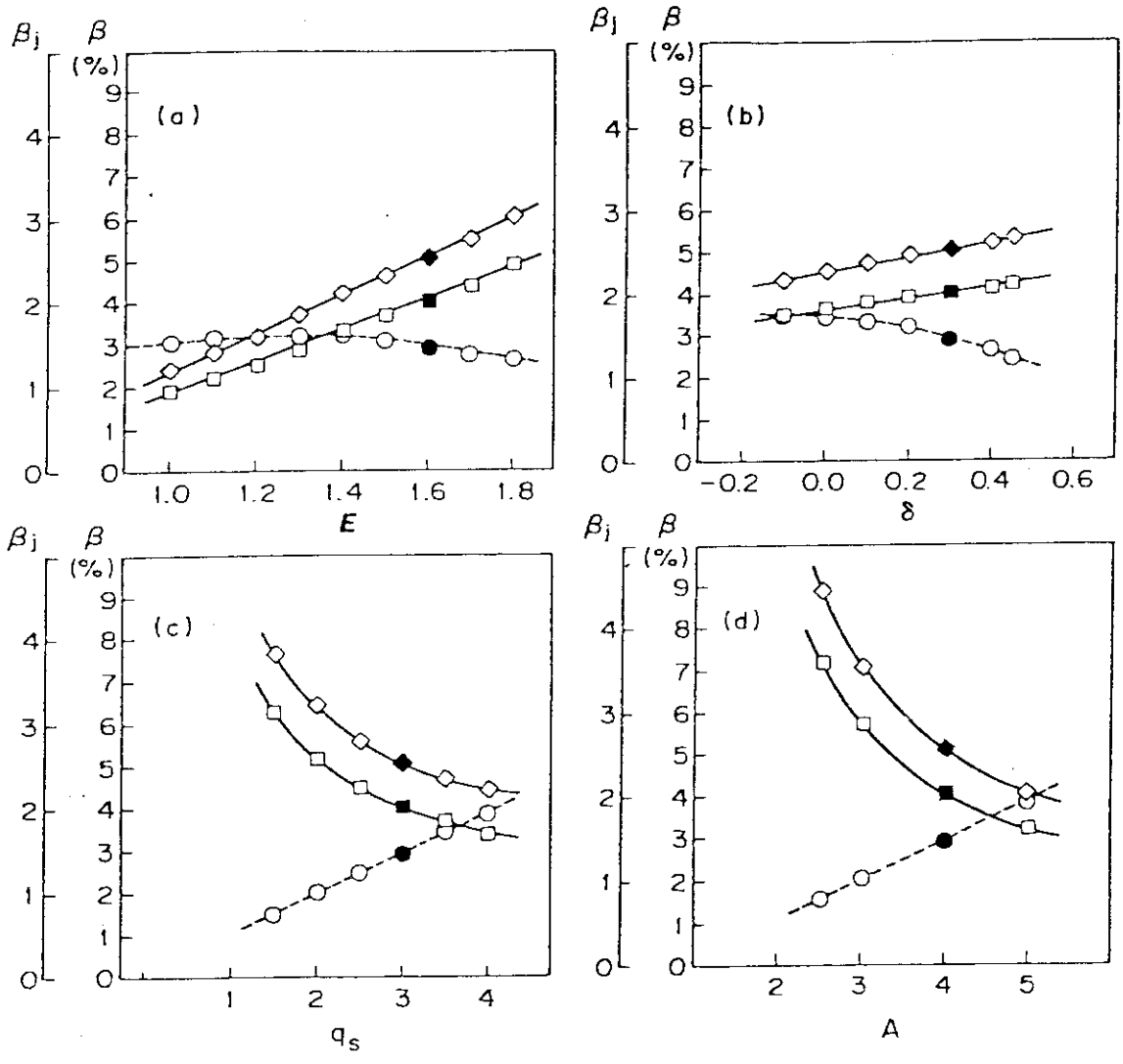

Fig. 6.5 Attainable β*(◇), β(□) and β_J(o), which are ballooning stable, versus (a) E:ellipticity, (b)δ:triangularity, (c) q_s:safety factor on the plasma surface and (d) A: aspect ratio. Black symbols correspond to standard INTOR parameters.

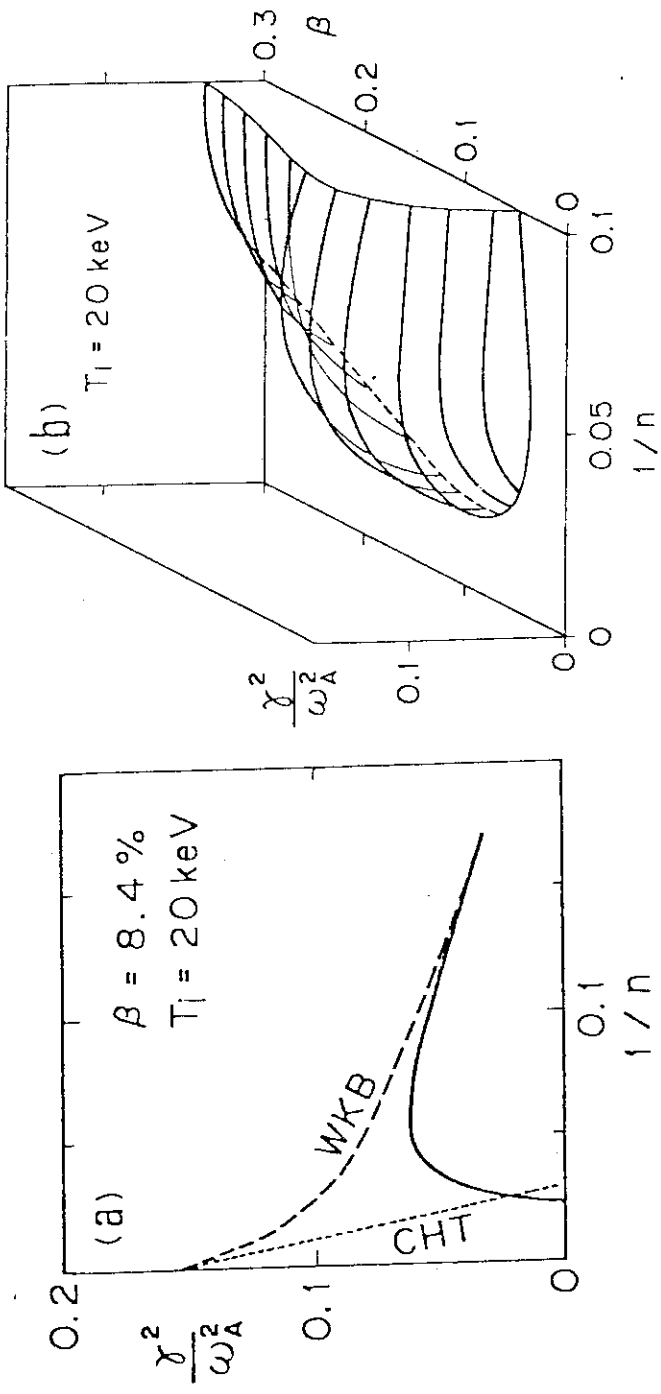

Fig. 6.6 (a) γ^2 versus 1/n. The dashed line denotes the MHD growth rate derived by WKB method and dotted line by CHT theory; the solid line shows $\gamma^2(n)$ with ω_* correction. (b) γ-n-β diagram: we see that the critical β is set by the mode with $n \geq 20$ and γ starts to decrease as β exceeds 12%.

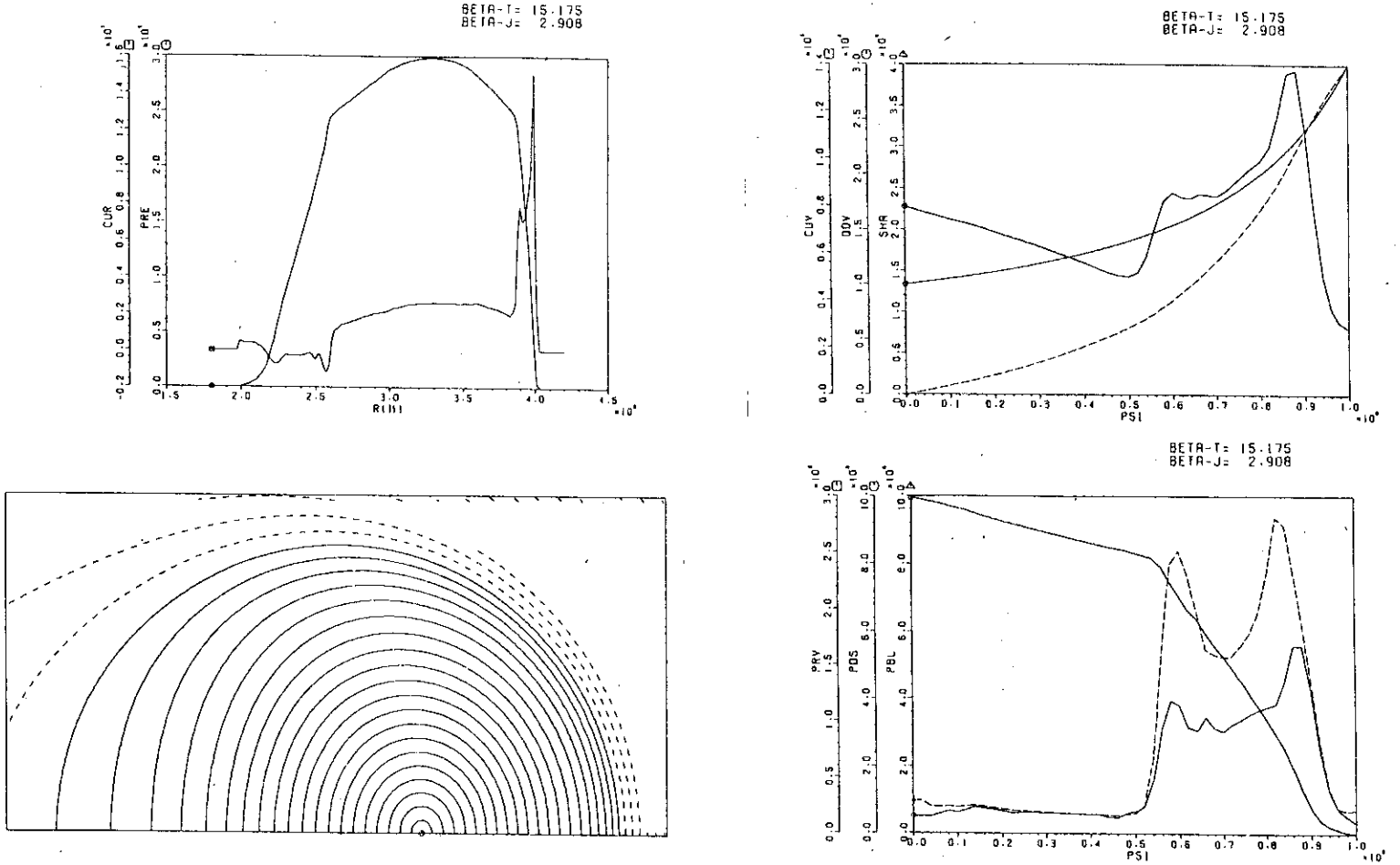

Fig. 6.7 An example of a second stable equilibrium with $\beta \simeq 15\%$, which is stable against the ballooning mode in a whole plasma region. CUV, QQV, and SHA are current density, safety factor, and shear as functions of ψ, respectively. PRV, PDS, and PBL are pressure (P), pressure gradient ($|\frac{dP}{d\psi}|$), and critical pressure gradient ($|\frac{dP}{d\psi}_{crit}|$) as functions of ψ, respectively. CUR and PRE are current density and pressure on the median plane as functions of radius, respectively.

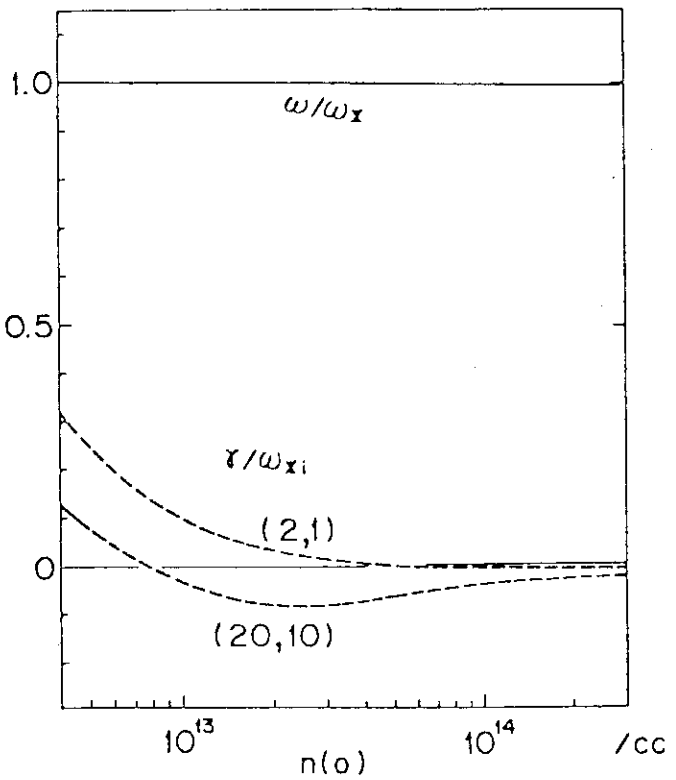

Fig. 7.1 Eigenvalues of (2,1) mode as a function of n(0). q(0)=1.49, q(a)=3.43, $a\Delta'$=12.1, T_e/T_i=2, T_e=4keV, η_J=1 and η_e=0. The growth rates are also shown for (20,10) mode. An n(0) exceeds 7×10^{13} cm^{-3}, the mode becomes stable.

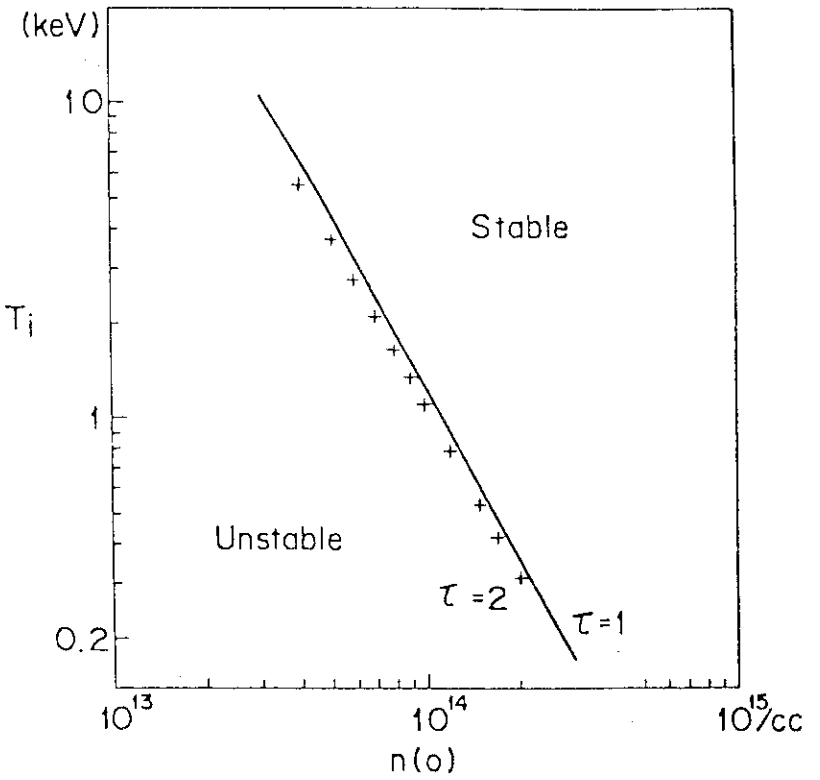

Fig. 7.2 Stability criterion for the parameters in Fig. 7.1. The solid line is for $\tau=T_e/T_i$=1 and + indicates τ=2 case.

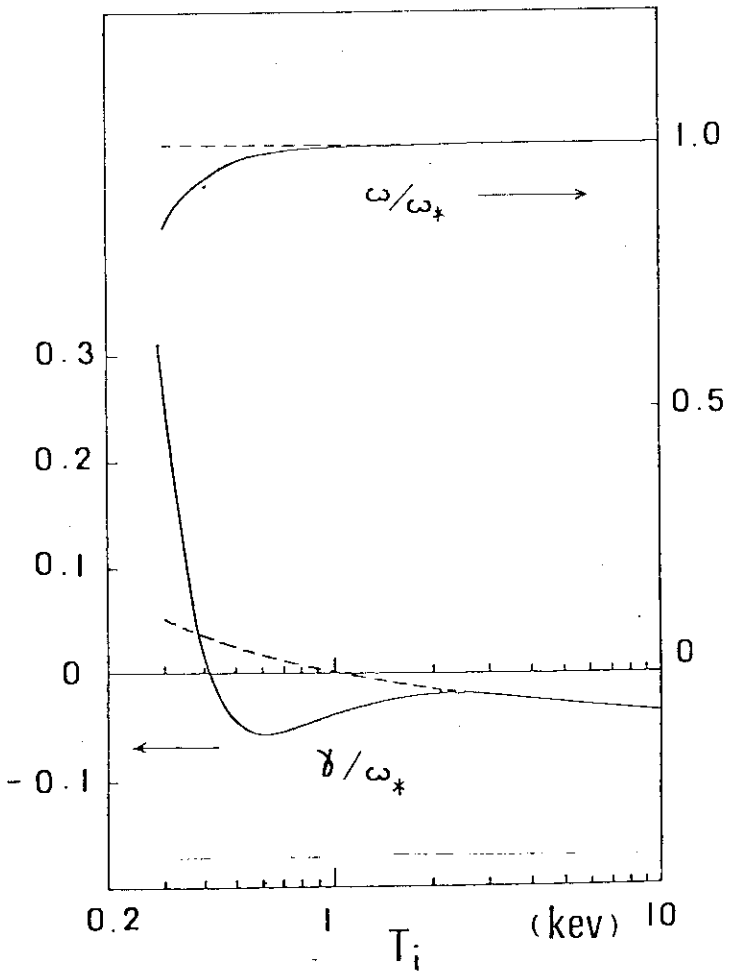

Fig. 7.3 Eigenvalues of the (2,1) kinetic tearing mode as a function of T_i. n(0) is chosen as $10^{14}cm^{-3}$ and other parameters are the same as in Fig.7.1. The solid line is due to the theory which keeps collisions and the dashed line is by the collisionless approximation.

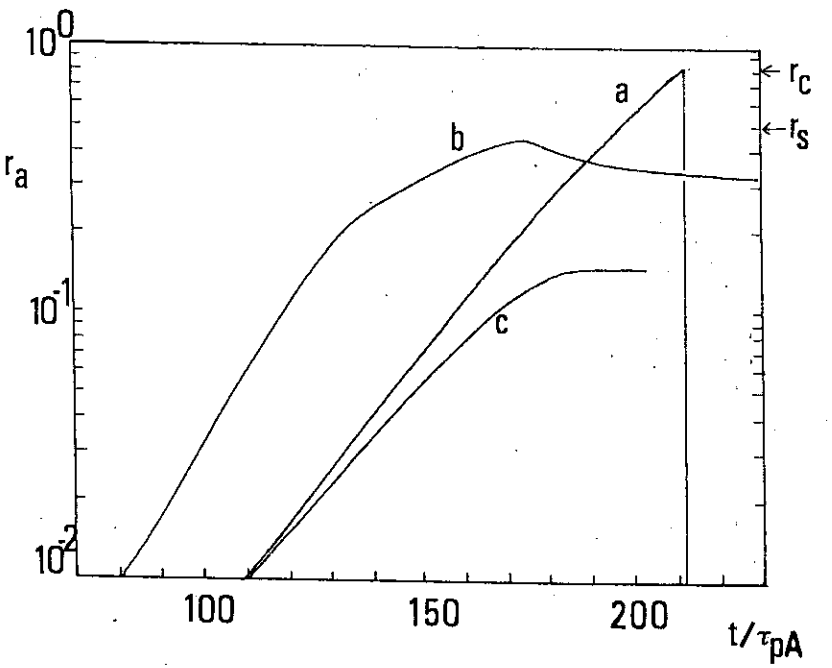

Fig. 7.4 Temporal change of the position of the magnetic axia r_a due to the resistive mode (a), resistive internal mode (b), and internal mode (c).

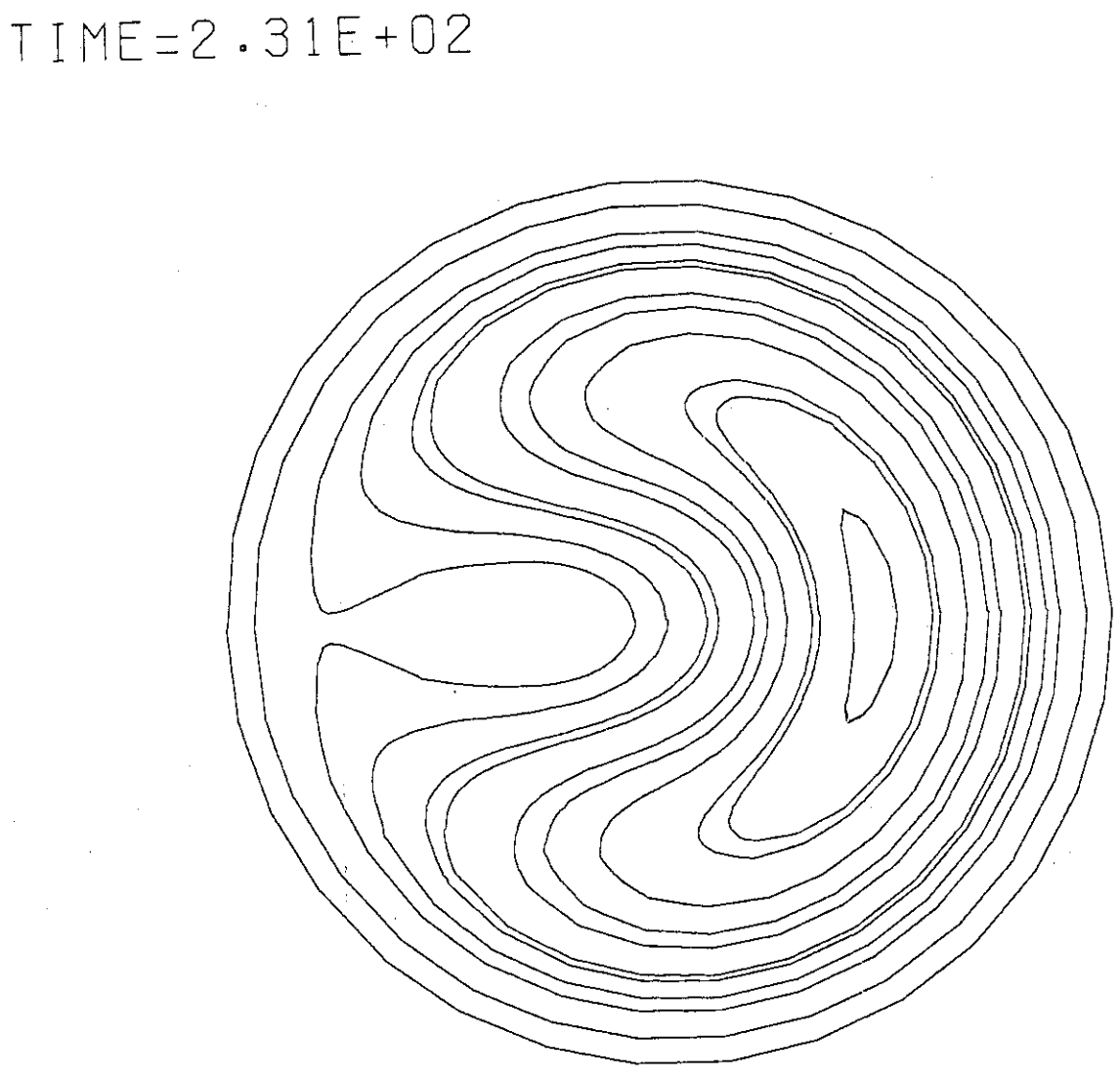

Fig. 7.5 Magnetic flux surfaces at the saturation level of the resistive internal mode.